Table 2 Clinical Characteristics of the Patients' Measurements of Hemodynamics at the Time of AMI (Baseline) and 6-Months' Follow-up

	Control group (n=36)	*PBMNC group (n=18)*	*p value*
LVSP (mmHg)			
Baseline	*121.7±13.0*	*120.3±13.9*	*0.73*
6 months	*125.0±19.2*	*126.9±8.7*	*0.67*
p value (baseline vs 6 months)	*0.47*	*0.10*	
LVDP (mmHg)			
Baseline	*3.9±4.8*	*4.6±5.1*	*0.67*
6 months	*3.1±2.4*	*4.1±3.5*	*0.27*
p value (baseline vs 6 months)	*0.4*	*0.73*	
LVEDP (mmHg)			
Baseline	*20.1±6.1*	*19.8±4.8*	*0.89*
6 months	*13.6±3.7*	*14.3±5.3*	*0.57*
p value (baseline vs 6 months)	*<0.0001*	*<0.0001*	
AOMP (mmHg)			
Baseline	*90.3±13.4*	*88.4±9.7*	*0.61*
6 months	*89.5±14.2*	*90.2±9.7*	*0.85*
p value (baseline vs 6 months)	*0.84*	*0.58*	
HR (beats/min)			
Baseline	*88.3±7.7*	*88.0±10.9*	*0.91*
6 months	*65.8±6.8*	*65.0±7.2*	*0.69*
p value (baseline vs 6 months)	*<0.0001*	*<0.0001*	

Values are mean±SD.
AMI, acute myocardial infarction; LVSP, left ventricular systolic pressure; LVDP, left ventricular diastolic pressure; LVEDP, left ventricular end-diastolic pressure; AOMP, aortic mean pressure; HR, heart rate. Other abbreviation see in Table 1.

Table 3 Clinical Characteristics of Patients' Baseline Cardiac Function

	Control group (n=36)	*PBMNC group (n=18)*	*p value*
LVEF (%)	*48.8±11.3*	*43.8±12.5*	*0.20*
EDVI (ml/m²)	*60.9±14.8*	*70.0±15.0*	*0.07*
ESVI (ml/m²)	*32.0±13.1*	*39.9±14.9*	*0.054*
Regional EF (%)			
Segment #2	*11.7±6.1*	*12.3±7.0*	*0.77*
Segment #3	*8.4±6.5*	*5.5±5.8*	*0.11*

LVEF, left ventricular ejection fraction; EDVI, end-diastolic volume index; ESVI, end-systolic volume index; EF, ejection fraction. Other abbreviation see in Table 1.

shown in Table 1. The PBMNC group and control group were well matched with respect to baseline characteristics and procedural characteristics, such as age, sex, and coronary risk factors, Killip class, infarct segment, and vessel diameter. Although particularly important factors influencing cardiac function are considered to be peak CK and time to revascularization, there were no significant differences in these factors between the 2 groups. All patients were treated with aspirin (100 mg/day), ticlopidine (200 mg/day for at least 4 weeks after PCI) or cilostazol (200 mg/day at least 4 weeks after PCI), statin, β-blocker, and angiotensin-converting enzyme inhibitor (ACEI) or angiotensin-receptor blocker (ARB) during the hospitalization for AMI and continued until the 6-months' follow-up examination, unless these agents were contraindicated. There were no significant differences between the control and PBMNC groups in the administration of ACEIs, ARBs, β-blockers or statins (Table 1).

No patient had either bleeding complications through the central venous access from the femoral vein or systemic blood pressure fall during the apheresis procedures. Although a transient further ST elevation associated with balloon occlusion was seen in the infarct-related ECG leads in most of the patients receiving PBMNCs, there were no serious symptomatic complaints or circulatory disturbances during or after cell transplantation. Neither intracoronary infusion nor the stop-flow procedure was performed in the control group. There were no fatal cardiac events during the follow-up period, and no patient in either group had any clinical manifestation of heart failure.

Endothelial Progenitors in AMI Patients

FACS analysis showed that the percentage of $CD34^+$ (0.12±0.2) or $CD34/KDR^+$ (0.05±0.1) cells in the PBMNCs from AMI patients tended to be higher (2–10-fold, but not statistically significant), compared with healthy volunteers ($CD34^+$; 0.06±0.1, $CD34/KDR^+$; 0.003±0.001), and that these cells also possess the characteristics of EPCs, as demonstrated by DiI-acetylated LDL uptake and lectin binding.

Hemodynamics and LV Function by Angiography

Table 2 shows the hemodynamic measurements in the control and PBMNC groups at the time of AMI (baseline) and at 6-months' follow-up. Although LV end-diastolic pressure (LVEDP) and heart rate (HR) were significantly reduced from baseline to 6-months' follow-up in both groups, there were no significant differences in LV systolic pressure (LVSP), LV diastolic pressure (LVDP), or aortic mean pressure (AOMP). Moreover, there were no statistically significant differences in LVSP, LVDP, LVEDP, AOMP, or HR between groups at either baseline or 6-months' follow-up.

Table 3 shows the clinical characteristics of baseline LV cardiac function. There were no significant differences in

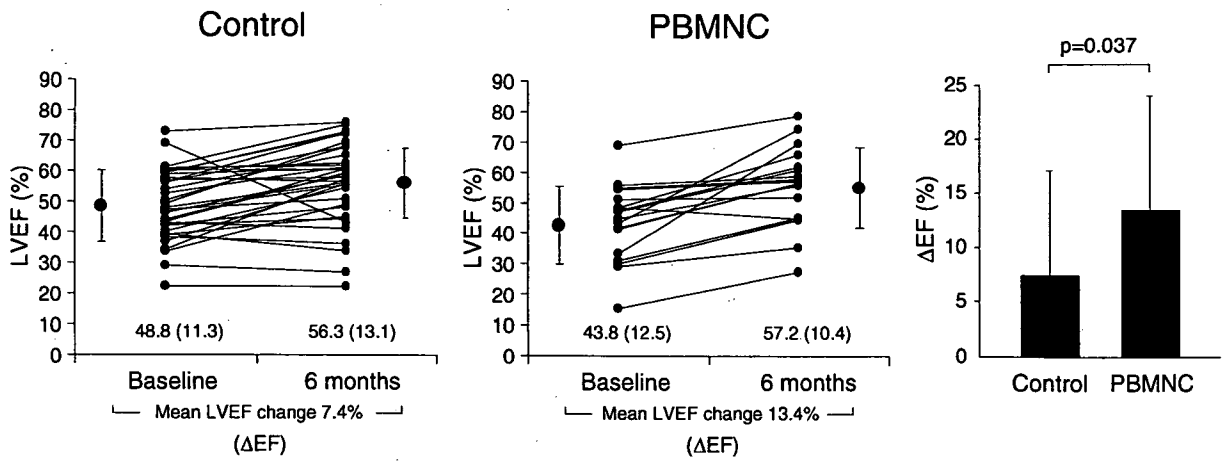

Fig 1. Global left ventricular ejection fraction (LVEF) at baseline and 6 months' follow-up, and the absolute increase in LVEF (Δejection fraction (EF)) in the control and peripheral blood mononuclear cell (PBMNC) groups. Small dots show data for individual patients; large dots show mean values. Vertical bars show SD.

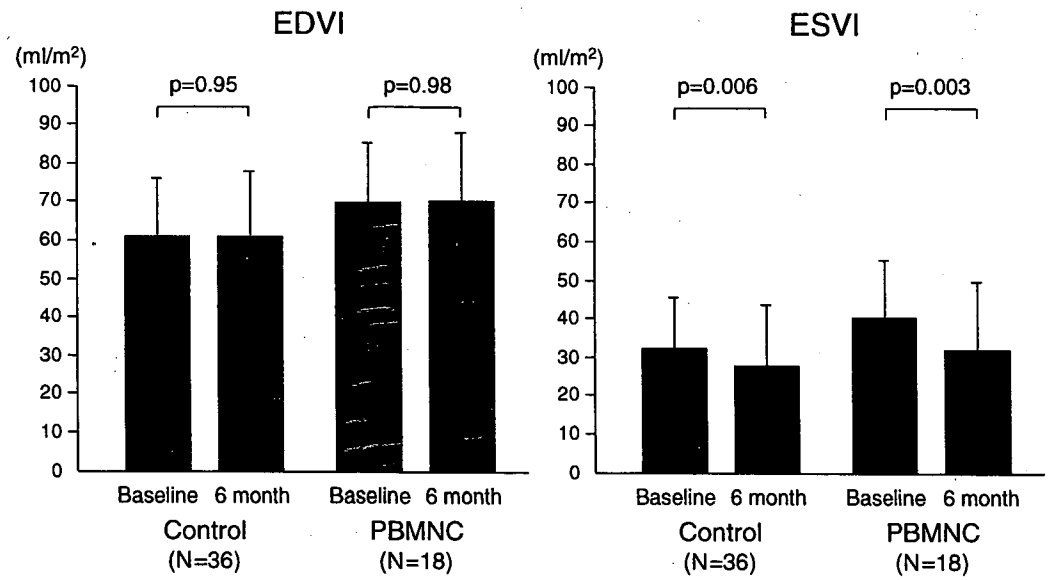

Fig 2. End-diastolic volume index (EDVI) and end-systolic volume index (ESVI) at baseline and 6 months' follow-up. Data are mean±SD. PBMNC, peripheral blood mononuclear cell.

LVEF, end-diastolic volume index (EDVI), end-systolic volume index (ESVI), or regional ejection fraction (EF) between the control and PBMNC groups. Fig 1 illustrates LV function as assessed by cineventriculography at baseline and 6-months' follow-up. In the control group, LVEF was 48.8% at baseline and gradually increased to 56.3% after 6 months. In contrast, LVEF was 43.8% at baseline and increased to 57.2% after 6 months in the PBMNC group. Although the baseline measurement of LVEF did not differ significantly between the 2 groups, the absolute increase in LVEF (ΔEF) was 7.4% in the control group and 13.4% in the PBMNC group. Our data therefore show that cell transplantation significantly improved LVEF, and there was a modest but significant increase in global LVEF, even in the patients with PCI alone (ie, controls). It is notable that the ΔEF value in thePBMNC group was significantly greater than that in the control group (PCI alone) (Fig 1).

There were no significant difference in EDVI between baseline and 6 months' follow-up in either control or PBMNC group (Fig 2) and also no significant difference in the absolute difference in EDVI (ΔEDVI) between the control and PBMNC groups (p=0.90). ESVI was significantly decreased from baseline to 6 months' follow-up in both groups, such that the absolute difference in ESVI (ΔESVI) was −4.3% in the control group and −8.2% in the PBMNC group. Thus, although there was no statistically significant difference in ΔESVI value between the 2 groups (p=0.09), the ΔESVI value tended to be lower in the PBMNC group, compared with controls. Selective analysis of the infarcted zone showed that baseline measurements of regional wall motion (regional EF), that is, segments #2 and #3 of the AHA classification, did not differ significantly between the control and PBMNC groups (Table 3). Although regional wall motion in the infarct area was significantly improved from baseline to 6 months' follow-up in both groups, the absolute value of regional EF (ΔRegional EF)

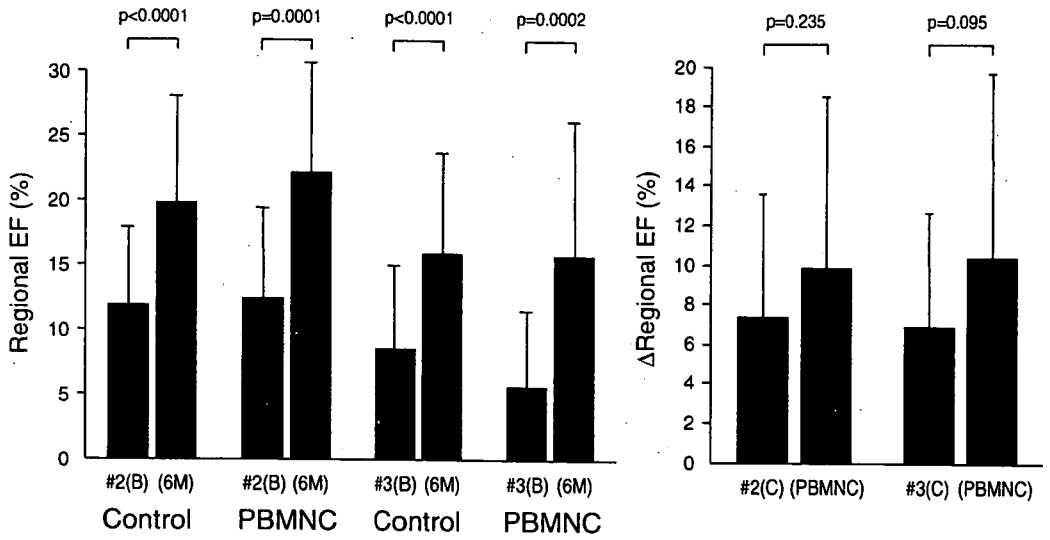

Fig 3. Regional ejection fraction (EF) at baseline and 6 months' follow-up, and the absolute increase in regional EF (ΔRegional EF) in the control and peripheral blood mononuclear cell (PBMNC) groups. Regional EF in the infarct area (segments #2 and #3) was estimated as described in Methods. Data are mean±SD.

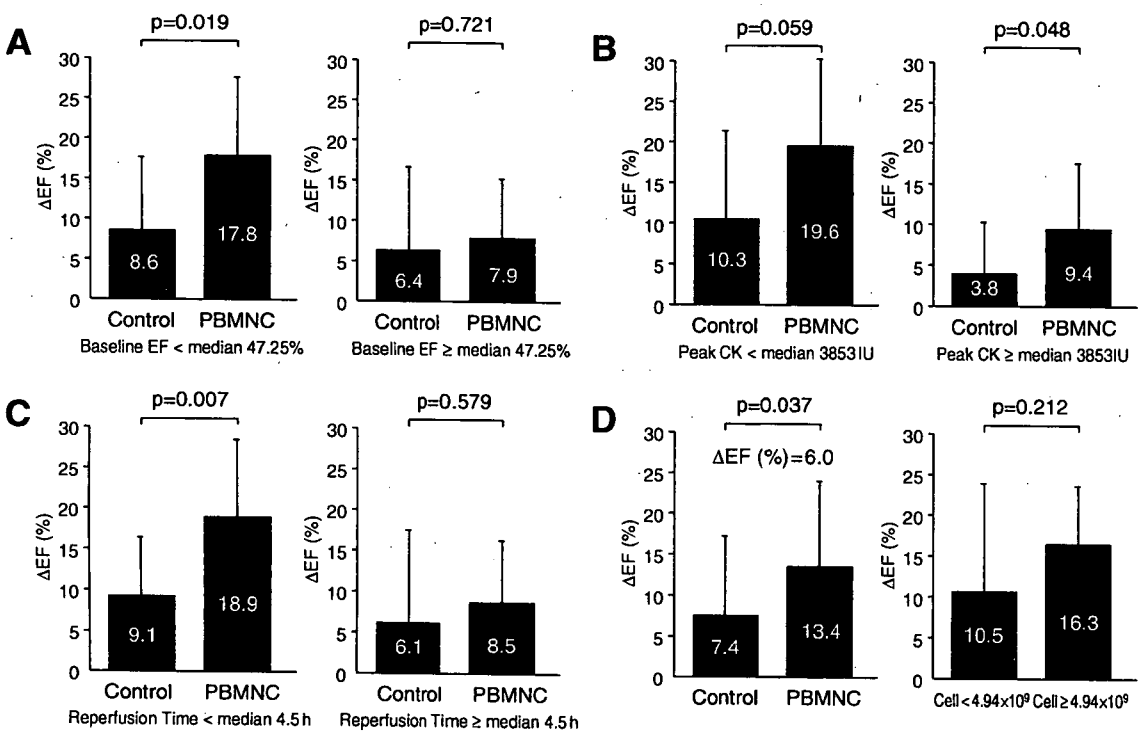

Fig 4. Impact of baseline ejection fraction (EF), peak creatine kinase (CK), reperfusion time, and transplanted cell number on cardiac function. All patients were divided into 2 groups by median baseline EF (A), median CK (B), median reperfusion time (C), and median transplanted cell number (D), and the treatment effect of peripheral blood mononuclear cell (PBMNC) infusion on the absolute increase in left ventricular EF (ΔEF) was analyzed. Data are mean±SD.3

tended to be greater in PBMNC group, compared with control (Fig 3).

Effects of Cell Transplantation on Other Parameters

Resting echocardiography indicated that cell transplantation significantly decreased the WMSI from baseline (1.67±0.18) to 6 months' follow-up (1.50±0.34) and this improvement in regional wall motion was especially seen in the infarct-related area of 15 of 18 patients. Resting ^{99m}Tc-tetrofosmin gated SPECT also showed that cell transplantation significantly decreased the perfusion defect score from baseline (20.4±9.0) to 6 months' follow-up (14.1±9.4), and this improvement in regional myocardial perfusion was seen in the infarct-related area of 14 of 18 patients. In con-

trast, cell transplantation did not significantly exacerbate but rather tend to decrease the Holter Lawn Class (data not shown).

Impact of Baseline Parameters and on Cardiac Function

We observed that cell transplantation significantly improved the ΔEF value, compared with controls (Fig 1). We further analyzed the effect of baseline parameters on the absolute increase in LVEF. In order to avoid our "arbitrary decision" on subgroup analysis, the total patient population was dichotomized according to the "median values" of baseline EF, peak CK, reperfusion time, and transplanted cell number at baseline, as previously reported[21] We then reanalyzed the data for addressing the clinical relevance of PBMNC administration.

We first examined the impact of baseline EF on cardiac function. When we divided all the patients into 2 groups by median baseline EF 47.25%, there was a significant interaction between the treatment effect of PBMNC infusion and the baseline EF. Among patients with a baseline EF below the median value, patients in the PBMNC group had an absolute increase in LVEF (ΔEF value) that was 2-fold that of the control group (Fig 4A) (absolute difference, 9.2%; 95% confidence interval (CI), 5.3 to 13.1). In contrast, among patients with a baseline EF at or above the median, the absolute difference between the 2 groups was only 1.5% (absolute difference, 1.5%; 95% CI, −2.1 to 5.1), suggesting that cell transplantation preferentially improved LV function in patients with relatively depressed contractility.

We next examined the impact of peak CK on cardiac function. When we divided all the patients into 2 groups by median peak CK 3,853 IU/dl, there was again a significant interaction between the treatment effect of PBMNC infusion and the peak CK. Among patients with a baseline peak CK at or above the median value, those in the PBMNC group had an absolute ΔEF value that was more than 2-fold the value for the control group (Fig 4B) (absolute difference, 5.6%; 95% CI, 2.8 to 8.4). Among patients with a baseline peak CK below the median, those in the PBMNC group also had an absolute ΔEF value that was ≈2-fold that in the control group, although there was not a significant difference in the ΔEF value between the 2 groups. The data suggest that cell transplantation preferentially improved LV function irrespective of infarct size.

We also examined the impact of reperfusion time on cardiac function. When we divided all the patients into 2 groups by a median reperfusion time of 4.5 h, there was again a significant interaction between the treatment effect of PBMNC infusion and the reperfusion time. Among patients with a baseline reperfusion time below the median value, those in the PBMNC group had an absolute ΔEF value that was almost 2-fold that in the control group (Fig 4C) (absolute difference, 9.8%; 95% CI, 6.1 to 13.5). In contrast, among patients with a baseline reperfusion time at or above the median, the absolute difference between the 2 groups was only 2.4% (absolute difference, 2.4%; 95% CI, −1.6 to 13.8), suggesting that cell transplantation preferentially improved LV function in patients with relatively early reperfusion.

We further examined the impact of transplanted cell number on cardiac function. When we divided the patients receiving cell therapy into 2 groups by a median cell number of 4.94×10^9, there was no significant interaction between the treatment effect of PBMNC infusion and the number of transplanted cells, suggesting that cell number did not significantly affect LV function, at least in our study (Fig 4D).

Clinical Manifestations and Adverse Effects

The occurrence of individual major adverse cardiac events of death, recurrence of myocardial infarction, or rehospitalization for heart failure did not differ significantly between the control and PBMNC groups. The rate of in-stent restenosis at the culprit lesion in patients who received PBMNC transplantation was 22.2%, which was not significantly different from that in the control patients (p=0.21).

Discussion

The major finding of the present study is that the intracoronary administration of non-expanded PBMNCs significantly enhanced the recovery of LV contractile function in patients optimally treated for AMI. After 6 months, the absolute increase in LVEF (ΔEF) was significantly higher in the PBMNC group than in controls. The enhanced recovery of LV contractile function after the administration of PBMNCs appeared to be related to a reduction in regional LV dysfunction within the territory of the infarct, because cell therapy resulted in a greater tendency of ΔRegional EF or significant improvement of WMSI and ^{99m}Tc-tetrofosmin perfusion defect score associated with the infarct area, compared with controls. Moreover, intracoronary administration of PBMNCs did not exacerbate LV expansion or high-risk arrhythmia after the infarction. Taken together, our findings indicate that when combined with optimal reperfusion therapy and standard medical treatment, intracoronary administration of PBMNCs is able to enhance the recovery of global and regional LV function after AMI.

Our results of subgroup analysis also provide some meaningful suggestions in the choice of patients for cell therapy against AMI; cell transplantation preferentially improved LV function in patients with relatively depressed contractility, irrespective of infarct size, and with relatively early reperfusion. Thus, patients with relatively early reperfusion and depressed LV contractile function had better improvement in contractile function after the intracoronary administration of PBMNCs. Our data therefore suggest that PBMNC transplantation may rescue dying myocytes that were severely stunned in the infarct border zone, irrespective of the infarct size.

Several lines of evidence suggest that the level of circulating CD34$^+$ EPCs is predictive of future cardiovascular events[30] and that bone marrow-derived CD34$^+$ cells could be important for cardiovascular repair[31] In the present study, we used a mean of 4.92×10^9 PBMNCs containing $\approx6\times10^6$ CD34$^+$ cells for intracoronary injection and obtained an increase of 6% in ΔEF value. In the BOOST and REPAIR-AMI trials, $\approx2.5\times10^9$ unfractionated BMCs and $\approx2.4\times10^8$ Ficoll-separated BMCs (≈2–3×10^6 CD34$^+$ cells) were transplanted, with increases of 6% and 2.5% in ΔEF values, respectively. In contrast, in Janssens's report and the ASTAMI trial, $\approx3\times10^8$ Ficoll-separated BMCs ($\approx2.8\times10^6$ CD34$^+$ cells) and $\approx7\times10^7$ Ficoll-separated BMCs ($\approx0.7\times10^6$ CD34$^+$ cells), respectively, were used, and there was no significant increase in ΔEF value. These data therefore indicate that the total number of injected cells or CD34$^+$ cells does not always correlate with the improvement in cardiac performance after cell transplantation, although trans-

planted cell numbers appear to have been relatively low in the ASTAMI trial. Indeed, cell number did not significantly affect LV function in our study (Fig4). Importantly, our study results also suggests that PBMNCs, which were even not culture-expanded, show great capability as a comparable cell source to BMCs.

In view of BMCs homing into the heart, the microenvironment (eg, niche) within the infarct tissue and the timing of cell delivery may be important for the incorporation of BMCs. Recent observations indicate that after intracoronary transfer only 1.3–2.6% of ^{18}F-FDG-labelled unselected BMMNCs were detected in the infarcted heart, whereas most cells homed into the liver and spleen within ≈1 h after intracoronary delivery[32] Therefore, the findings do not support the likelihood that progenitor cells home into jeopardized myocardium and transdifferentiate into cardiac myocytes capable of generating active force development in scar tissue, but rather suggest other potential mechanisms through angiogenesis and reduced apoptosis. Indeed, recent articles have shed light on the potential of BMCs to differentiate into hematopoietic and endothelial lineages able to secrete proangiogenic factors[33] rather than transdifferentiation into other cell lineages such as cardiac myocytes[34,35] These subsets of mature hematopoietic cells, either derived from bone marrow or peripheral blood, may cooperate with transplanted or resident cardiac and endothelial stem/progenitor cells to enhance their capacity for tissue repair through angiogenesis, anti-apoptosis, and myocyte proliferation after ischemic injury[36,37]

The most potential advantage of our method is its feasibility and safety in collecting PBMNCs from patients with depressed cardiac performance and bleeding tendency, by administration of enough antiplatelet agents, such as aspirin and ticlopidine. Although previous studies emphasize the feasibility and safety of BMCs aspiration, this maneuver is always accompanied by the risk of s serious bleeding accident from bone in patients receiving antiplatelet therapy. There are also a few other reports indicating a benefit of intracoronary infusion of granulocyte colony-stimulating factor (G-CSF) mobilized-PBMNCs for AMI[38–40] However, this procedure still involves several possible adverse effects of G-CSF, including serious thrombosis, bone pain, fever, and aggravation of in-stent restenosis[38–40] In contrast to those previous studies, we could easily collect ≈5×10^9 cells PBMNCs, avoiding contamination with neutrophils, within 2 h without any hemodynamic or bleeding problems. We could concentrate the collected PBMNCs to 10 ml by density gradient centrifugation aseptically through bag to bag, instead of by Ficoll gradient sedimentation methods. Our present data, therefore, show for the first time that intracoronary infusion of non-expanded PBMNCs alone can promote improvement of LV function without any bleeding accident or G-CSF-related serious adverse effects. Because we can easily obtain levels of ≈6×10^6 CD34$^+$ cells, which is higher than in either the BOOST or REPAIR-AMI trials, we never need another laboratory to expand the PBMNCs, giving substantial merit that this protocol can be easily accepted in any hospital worldwide.

A major limitation of our study is that evaluation of the present regeneration therapy was not randomized, double-blind, and controlled. Moreover, cardiac function was not assessed with state-of-the-art imaging modalities, such as magnetic resonance imaging (MRI), and LV angiography was used exclusively for the serial assessment of LV function. Although angiography is well suited to delineate regional contractile function for AMI by LAD occlusion, the use of MRI to assess global LV function would have more precisely depicted changes in the distorted geometry of the infarcted hearts. Although we choose contemporary controls, the control group does not reproduce the exact conditions of the cell therapy group to which the cells were transferred, including PBMNC collection and a placebo intracoronary injection. Therefore, the true benefit of cell transfer can not be fully appreciated and further research is needed to address these issues.

In conclusion, intracoronary infusion of PBMNCs in patients with AMI is associated with improved global LV contractile function; cell therapy preferentially improves LV function in patients with early reperfusion, but relatively depressed contractility after AMI, prevents end-diastolic and end-systolic LV volume expansion, and has not increased any adverse clinical events so far. Transplantation of PBMNCs might be an effective and novel therapeutic option for AMI, if cell transfer occurs expeditiously and in appropriate subjects. This less invasive and more feasible approach to collecting EPCs may be a novel therapeutic option for improving cardiac function after AMI.

Acknowledgments

This study was supported in part by Grants-in-Aid from the Ministry of Education, Culture, Sports, Science and Technology and from the Ministry of Health, Labor and Welfare in Japan.

References

1. Cleaver O, Melton DA. Endothelial signaling during development. *Nat Med* 2003; **9:** 661–668.
2. Asahara T, Murohara T, Sullivan A, Silver M, van der Zee R, Li T, et al. Isolation of putative progenitor endothelial cells for angiogenesis. *Science* 1997; **275:** 964–967.
3. Asahara T, Takahashi T, Masuda H, Kalka C, Chen D, Iwaguro H, et al. VEGF contributes to postnatal neovascularization by mobilizing bone marrow-derived endothelial progenitor cells. *EMBO J* 1999; **18:** 3964–3972.
4. Asahara T, Kawamoto A. Endothelial progenitor cells for postnatal vasculogenesis. *Am J Physiol Cell Physiol* 2004; **287:** C572–C579.
5. Kamihata H, Matsubara H, Nishiue T, Fujiyama S, Tsutsumi Y, Ozono R, et al. Implantation of bone marrow mononuclear cells into ischemic myocardium enhances collateral perfusion and regional function via side supply of angioblasts, angiogenic ligands, and cytokines. *Circulation* 2001; **104:**1046–1052.
6. Qin SL, Li TS, Takahashi M, Hamano K. In vitro assessment of the effect of interleukin-1beta on angiogenic potential of bone marrow cells. *Circ J* 2006; **70:** 1195–1199.
7. Tateishi-Yuyama E, Matsubara H, Murohara T, Ikeda U, Shintani S, Masaki H, et al; Therapeutic Angiogenesis using Cell Transplantation (TACT) Study Investigators. Therapeutic angiogenesis for patients with limb ischaemia by autologous transplantation of bone-marrow cells: A pilot study and a randomised controlled trial. *Lancet* 2002; **360:** 427–435.
8. Goodell MA, Jackson KA, Majka SM, Mi T, Wang H, Pocius J, et al. Stem cell plasticity in muscle and bone marrow. *Ann NY Acad Sci* 2001; **938:** 208–218.
9. Quaini F, Urbanek K, Beltrami AP, Finato N, Beltrami CA, Nadal-Ginard B, et al. Chimerism of the transplanted heart. *N Engl J Med* 2002; **346:** 5–15.
10. Fukuda K. Progress in myocardial regeneration and cell transplantation. *Circ J* 2005; **69:** 1431–1446.
11. Leor J, Patterson M, Quinones MJ, Kedes LH, Kloner RA. Transplantation of fetal myocardial tissue into the infarcted myocardium of rat: A potential method for repair of infarcted myocardium? *Circulation* 1996; **94:** II-332–II-336.
12. Murry CE, Wiseman RW, Schwartz SM. Hauschka SD. Skeletal myoblast transplantation for repair of myocardial necrosis. *J Clin Invest* 1996; **98:** 2512–2523.
13. Taylor DA, Atkins BZ, Hungspreugs P, Jones TR, Reedy MC, Hutcheson KA, et al. Regenerating functional myocardium: Improved performance after skeletal myoblast transplantation. *Nat Med* 1998; **4:** 929–933.

14. Orlic D, Kajstura J, Chimenti S, Jakoniuk I, Anderson SM, Li B, et al. Bone marrow cells regenerate infarcted myocardium. *Nature* 2001; **410:** 701–705.
15. Orlic D, Kajstura J, Chimenti S, Limana F, Jakoniuk I, Quaini F, et al. Mobilized bone marrow cells repair the infarcted heart, improving function and survival. *Proc Natl Acad Sci USA* 2001; **98:** 10344–10349.
16. Stamm C, Westphal B, Kleine HD, Petzsch M, Kittner C, Klinge H, et al. Autologous bone-marrow stem-cell transplantation for myocardial regeneration. *Lancet* 2003; **361:** 45–46.
17. Tse HF, Kwong YL, Chan JK, Lo G, Ho CL, Lau CP. Angiogenesis in ischaemic myocardium by intramyocardial autologous bone marrow mononuclear cell implantation. *Lancet* 2003; **361:** 47–49.
18. Strauer BE, Brehm M, Zeus T, Kostering M, Hernandez A, Sorg RV, et al. Repair of infarcted myocardium by autologous intracoronary mononuclear bone marrow cell transplantation in humans. *Circulation* 2002; **106:** 1913–1918.
19. Assmus B, Schachinger V, Teupe C, Britten M, Lehmann R, Dobert N, et al. Transplantation of Progenitor Cells and Regeneration Enhancement in Acute Myocardial Infarction (TOPCARE-AMI). *Circulation* 2002; **106:** 3009–3017.
20. Wollert KC, Meyer GP, Lotz J, Ringes-Lichtenberg S, Lippolt P, Breidenbach C, et al. Intracoronary autologous bone-marrow cell transfer after myocardial infarction: The BOOST randomised controlled clinical trial. *Lancet* 2004; **364:** 141–148.
21. Schachinger V, Erbs S, Elsasser A, Haberbosch W, Hambrecht R, Holschermann H, et al; REPAIR-AMI Investigators. Intracoronary bone marrow-derived progenitor cells in acute myocardial infarction. *N Engl J Med* 2006; **355:** 1210–1221.
22. Lunde K, Solheim S, Aakhus S, Arnesen H, Abdelnoor M, Egeland T, et al. Intracoronary injection of mononuclear bone marrow cells in acute myocardial infarction. *N Engl J Med* 2006; **355:** 1199–1209.
23. Janssens S, Dubois C, Bogaert J, Theunissen K, Deroose C, Desmet W, et al. Autologous bone marrow-derived stem-cell transfer in patients with ST-segment elevation myocardial infarction: Double-blind, randomised controlled trial. *Lancet* 2006; **367:** 113–121.
24. Kamihata H, Matsubara H, Nishiue T, Fujiyama S, Amano K, Iba O, et al. Improvement of collateral perfusion and regional function by implantation of peripheral blood mononuclear cells into ischemic hibernating myocardium. *Arterioscler Thromb Vasc Biol* 2002; **22:** 1804–1810.
25. Iba O, Matsubara H, Nozawa Y, Fujiyama S, Amano K, Mori Y, et al. Angiogenesis by implantation of peripheral blood mononuclear cells and platelets into ischemic limbs. *Circulation* 2002; **106:** 2019–2025.
26. Shintani S, Murohara T, Ikeda H, Ueno T, Honma T, Katoh A, et al. Mobilization of endothelial progenitor cells in patients with acute myocardial infarction. *Circulation* 2001; **103:** 2776–2779.
27. Askari AT, Unzek S, Popovic ZB, Goldman CK, Forudi F, Kiedrowski M, et al. Effect of stromal-cell-derived factor 1 on stem-cell homing and tissue regeneration in ischaemic cardiomyopathy. *Lancet* 2003; **362:** 697–703.
28. Halkin A, Stone GW, Grines CL, Cox DA, Rutherford BD, Esente P, et al. Prognostic implications of creatine kinase elevation after primary percutaneous coronary intervention for acute myocardial infarction. *J Am Coll Cardiol* 2006; **47:** 951–961.
29. Katayama T, Nakashima H, Takagi C, Honda Y, Suzuki S, Iwasaki Y, et al. Prognostic significance of time-delay to peak creatine kinase after direct percutaneous coronary intervention in acute myocardial infarction patients. *Int Heart J* 2005; **46:** 607–618.
30. Werner N, Kosiol S, Schiegl T, Ahlers P, Walenta K, Link A, et al. Circulating endothelial progenitor cells and cardiovascular outcomes. *N Engl J Med* 2005; **353:** 999–1007.
31. Yeh ET, Zhang S, Wu HD, Korbling M, Willerson JT, Estrov Z. Transdifferentiation of human peripheral blood CD34$^+$-enriched cell population into cardiomyocytes, endothelial cells, and smooth muscle cells in vivo. *Circulation* 2003; **108:** 2070–2073.
32. Hofmann M, Wollert KC, Meyer GP, Menke A, Arseniev L, Hertenstein B, et al. Monitoring of bone marrow cell homing into the infarcted human myocardium. *Circulation* 2005; **111:** 2198–2202.
33. Heil M, Ziegelhoeffer T, Mees B, Schaper W. A different outlook on the role of bone marrow stem cells in vascular growth: Bone marrow delivers software not hardware. *Circ Res* 2004; **94:** 573–574.
34. Murry CE, Soonpaa MH, Reinecke H, Nakajima H, Nakajima HO, Rubart M, et al. Haematopoietic stem cells do not transdifferentiate into cardiac myocytes in myocardial infarcts. *Nature* 2004; **428:** 664–668.
35. Balsam LB, Wagers AJ, Christensen JL, Kofidis T, Weissman IL, Robbins RC. Haematopoietic stem cells adopt mature haematopoietic fates in ischaemic myocardium. *Nature* 2004; **428:** 668–673.
36. Kocher AA, Schuster MD, Szabolcs MJ, Takuma S, Burkhoff D, Wang J, et al. Neovascularization of ischemic myocardium by human bone-marrow-derived angioblasts prevents cardiomyocyte apoptosis, reduces remodeling and improves cardiac function. *Nat Med* 2001; **7:** 430–436.
37. Wollert KC, Drexler H. Clinical applications of stem cells for the heart. *Circ Res* 2005; **96:** 151–163.
38. Kang HJ, Kim HS, Zhang SY, Park KW, Cho HJ, Koo BK, et al. Effects of intracoronary infusion of peripheral blood stem-cells mobilised with granulocyte-colony stimulating factor on left ventricular systolic function and restenosis after coronary stenting in myocardial infarction: The MAGIC cell randomised clinical trial. *Lancet* 2004; **363:** 751–756.
39. Kang HJ, Lee HY, Na SH, Chang SA, Park KW, Kim HK, et al. Differential effect of intracoronary infusion of mobilized peripheral blood stem cells by granulocyte colony-stimulating factor on left ventricular function and remodeling in patients with acute myocardial infarction versus old myocardial infarction: The MAGIC Cell-3-DES randomized, controlled trial. *Circulation* 2006; **114:** I-145–I-151.
40. Li ZQ, Zhang M, Jing YZ, Zhang WW, Liu Y, Cui LJ, et al. The clinical study of autologous peripheral blood stem cell transplantation by intracoronary infusion in patients with acute myocardial infarction (AMI). *Int J Cardiol* 2007; **115:** 52–56.

Clonally amplified cardiac stem cells are regulated by Sca-1 signaling for efficient cardiovascular regeneration

Kento Tateishi[1,2], Eishi Ashihara[1], Naofumi Takehara[1], Tetsuya Nomura[1,2], Shoken Honsho[2], Takuo Nakagami[2,3], Shigehiro Morikawa[4], Tomosaburo Takahashi[1,2], Tomomi Ueyama[1], Hiroaki Matsubara[1,2,*] and Hidemasa Oh[1,*]

[1]Department of Experimental Therapeutics, Translational Research Center, Kyoto University Hospital, Kyoto 606-8507, Japan
[2]Department of Cardiovascular Medicine, [3]Departments of Pathology and Cell Regulation, Kyoto Prefectural University of Medicine, Kyoto 602-8566, Japan
[4]Molecular Neuroscience Research Center, Shiga University of Medical Science, Shiga 520-2192, Japan
*Authors for correspondence (e-mail: matsubah@koto.kpu-m.ac.jp; hidemasa@kuhp.kyoto-u.ac.jp)

Accepted 25 March 2007
Journal of Cell Science 120, 1791-1800 Published by The Company of Biologists 2007
doi:10.1242/jcs.006122

Summary

Recent studies have shown that cardiac stem cells (CSCs) from the adult mammalian heart can give rise to functional cardiomyocytes; however, the definite surface markers to identify a definitive single entity of CSCs and the molecular mechanisms regulating their growth are so far unknown. Here, we demonstrate a single-cell deposition analysis to isolate individually selected CSCs from adult murine hearts and investigate the signals required for their proliferation and survival. Clonally proliferated CSCs express stem cell antigen-1 (Sca-1) with embryonic stem (ES) cell-like and mesenchymal cell-like characteristics and are associated with telomerase reverse transcriptase (TERT). Using a transgene that expresses a GFP reporter under the control of the TERT promoter, we demonstrated that $TERT^{GFP}$-positive fractions from the heart were enriched for cells expressing Sca-1. Knockdown of Sca-1 transcripts in CSCs led to retarded ex vivo expansion and apoptosis through Akt inactivation. We also show that ongoing CSC proliferation and survival after direct cell-grafting into ischemic myocardium require Sca-1 to upregulate the secreted paracrine effectors that augment neoangiogenesis and limit cardiac apoptosis. Thus, Sca-1 might be an essential component to promote CSC proliferation and survival to directly facilitate early engraftment, and might indirectly exert the effects on late cardiovascular differentiation after CSC transplantation.

Key words: Cardiac stem cells, Proliferation, Regeneration, Stem cell antigen-1, Survival, Telomerase

Introduction

The adult mammalian heart harbors a population of mitotically competent cardiac stem cells (CSCs) that can be isolated by using FACS to recognize the cells expressing surface antigens KIT and stem cell antigen-1 (Sca-1) or by targeting a reporter gene driven by the promoter for islet-1, a LIM-homeodomain transcription factor (Beltrami et al., 2003; Laugwitz et al., 2005; Matsuura et al., 2004; Moretti et al., 2006; Oh et al., 2003; Pfister et al., 2005). These cells express essential cardiac transcriptional factors but do not express more mature markers of structural genes; however, the exact contribution of cell fusion in the process of adopting cardiac muscle phenotype after cell transfer into ischemic myocardium remains controversial (Beltrami et al., 2003; Oh et al., 2003). Within the adult heart, CSCs often reside in cardiac niches with supporting cells that provide a specialized environment to replenish and maintain a balance of survival, proliferation and self-renewal of CSCs through symmetric or asymmetric division in order to replace the mature cells that are lost during injury or turnover (Urbanek et al., 2006).

The general lack of definitive molecular markers to identify cardiac stem cells raises the fundamental question of whether these cardiac stem cells are derived from a single entity. CSCs in the mammalian heart share several cell-surface markers with hematopoietic and endothelial progenitor cells (Linke et al., 2005; Messina et al., 2004; Urbanek et al., 2003). Although the hierarchies of hematopoietic stem cells have been well characterized, evidence supporting the role of bone marrow-derived Lin^{-}-Kit^{+} cells in cardiac-lineage induction has been controversial (Kawada et al., 2004; Murry et al., 2004; Orlic et al., 2001). Recent reports have demonstrated that genetic disruption of *Kit* in mice mainly affects marrow-derived hematopoietic and endothelial cell development for cardiac repair, that could be rescued by bone marrow replacement with wild-type cells, through the failure of progenitor-cell mobilization from marrow and reduced release of cytokines and chemokines that may participate in the cardioprotective paracrine signaling (Ayach et al., 2006; Fazel et al., 2006). These studies do not exclude the possible functional role of KIT in resident CSCs as the principal mediator in the regenerating process during cardiac injury, but suggest that defining CSCs using specific cell-surface markers may not be optimal to address the identity of these cells, as indicated by their partially overlapping expression in human hearts (Urbanek et al., 2005b).

Decline of CSC function may be a major cause of the decrease in regenerative capacity in aging and disease (Rota et al., 2006). Although some of the growth factors involved in *Kit*$^{+}$ CSC proliferation and survival have been identified, factors regulating *Kit*$^{-}$ CSCs have yet to be defined (Gude et al., 2006; Limana et al., 2005; Urbanek et al., 2005a). In this study, we sought to identify single proliferative cells from the adult heart without progenitor selection using particular surface markers. Using this unbiased approach, we have established clonal CSC lines and demonstrated that the majority of the telomerase-active progenitor-cell colonies expressed Sca-1 and showed mesenchymal-cell-like character. We also show that targeting the Sca-1 transcripts in CSCs used for cell grafting leads to failure of their ability to prevent cardiac remodeling after myocardial infarction. The antiapoptotic and angiogenetic paracrine activities of intrinsic Sca-1 signaling in CSCs promote direct CSC proliferation and survival, and contribute to neovascularization in the host myocardium for efficient cardiovascular regeneration.

Results

Clonal isolation of cardiac stem cells in the adult heart

To identify the single entity of CSCs in the adult heart, we employed an unbiased approach using a single-cell clonogenic isolation technique to isolate a proliferative cell population. Singly dissociated GFP-labelled transgenic cells derived from the hearts of GFP transgenic mice were plated at a density of one cell per well in serum-free medium (Fig. 1A,B). Altogether, 11,520 single cells were deposited, and from 9541 single cells determined by inspection on day 1 to be present as one individual cell per well, a total of 11 clones arose within 7 days. Eight out 11 clones failed to grow in serum-free medium after 7 days in culture, and 3 clones (~0.03%) could proliferate to form spherical clusters and were continuously expanded after 14 days (Fig. 1C). The three independent colonies were re-dissociated and re-plated in low-serum for expansion, and individual CSC colonies were used for the following experiments to characterize clonal CSCs.

Characterization of clonally amplified CSCs

Immunophenotyping revealed that the clonal CSCs strongly expressed Sca-1, which is used as a marker to identify cardiac progenitor cells from the adult heart (Matsuura et al., 2004; Oh et al., 2003), whereas KIT-positive cells were rarely detected (Fazel et al., 2006; Gude et al., 2006; Pfister et al., 2005) (Fig. 1D). Notably, CSCs did not express the hematopoietic and endothelial progenitor-cell-specific surface antigens CD45, CD34 and CD31, but did express the typical mesenchymal stem-cell surface antigens CD90, CD105, CD29, CD44, CD106, CD73 and CD13 (Pittenger and Martin, 2004). The three individual CSCs exhibited an identical immunophenotyping for the surface marker analysis. The cell membrane antigens Sca-1, KIT, CD45, and CD34 were not destroyed by collagenase treatment as tested in bone marrow (data not shown).

Gene expression was then examined in CSC clones using reverse transcriptase (RT)-PCR (Fig. 1E). Three individual colonies were analyzed and most of the clones expressed Bcrp1, polycomb group protein Bmi1 and also telomerase reverse transcriptase (TERT), which has been reported to be absent in cardiac fibroblasts (Leri et al., 2001). Although Nanog was detectable in all of the colonies examined, none of the colonies – unlike embryonic stem (ES) cells – were positive for OCT4 or UTF1. Some but not all of the colonies expressed HNF3β, brachyury and SOX2, which are endodermal, mesodermal and ectodermal precursor markers, respectively. These results distinguished clonal CSCs from mouse fibroblasts, which are negative for all of the ES cell markers described above (Takahashi and Yamanaka, 2006). In addition, all of the colonies analyzed expressed nestin, a marker of immature neural progenitor cells (Joannides et al., 2004).

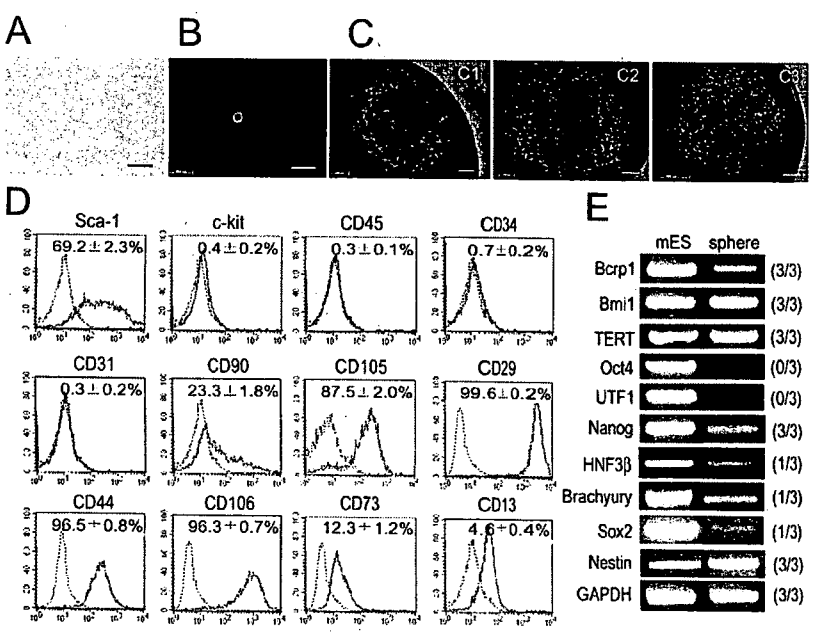

Fig. 1. Clonal isolation and characterization of stem cells in the adult heart. (A,B) Single-cell deposition analysis was performed by the limiting dilution technique. At day 1 of the culture period, wells were inspected for the presence of single cells by phase contrast (A) and GFP fluorescence (B). (C) Colony formation from single cells in 96-well plates at 14 days of culture in serum-free medium. Three-independent colonies derived from single cells are shown. (D) FACS analysis of CSCs. Black line, control IgG; red line, corresponding antibody. Data are representative of three independent clonal CSCs. (E) RT-PCR for CSC clones. The numbers on the right indicate the number of individual colonies that expressed the corresponding genes out of the colonies examined. mES, mouse ES cells used as positive control. Data are representative of three independent clonal CSCs. Bars, 20 μm in A,B; 500 μm in C.

TERT-expressing cells in postnatal heart are associated with Sca-1 expression

TERT has been identified as a key factor controlling telomerase activity, telomere length, and cell growth (Blackburn, 2001). We measured the telomerase activity in clonal CSCs. The three individual CSCs displayed significantly elevated telomerase activity (Fig. 2A). To directly characterize TERT-expressing cells in the adult heart, we engineered transgenic mice expressing enhanced green fluorescent protein (EGFP) under the control of the mouse *Tert* promoter (Fig. 2B). We identified two transgenic founders by genomic DNA screening and established two independent lines (Fig. 2C). In order to examine the efficacy of mouse *Tert* promoter in the heart in vivo, cells isolated from transgenic hearts were sorted by EGFP signal and the EGFP-positive cells were found to be TERT-expressing cells, which were not detectable in EGFP$^-$ populations (Fig. 2D). As expected from high telomerase activities of clonal CSCs shown in Fig. 2A, three individual CSC clones showed TERT expression (Fig. 2D). To further characterize the TERT-positive cells in the heart, FACS analysis was performed. FACS of the cells prepared from the heart of adult mice expressing TERT-EGFP indicated that TERT^{GFP}-positive cells constitute a population that is positive for Sca-1 but rarely expressing detectable levels of c-kit, CD45, CD34, or CD31 (Fig. 2E).

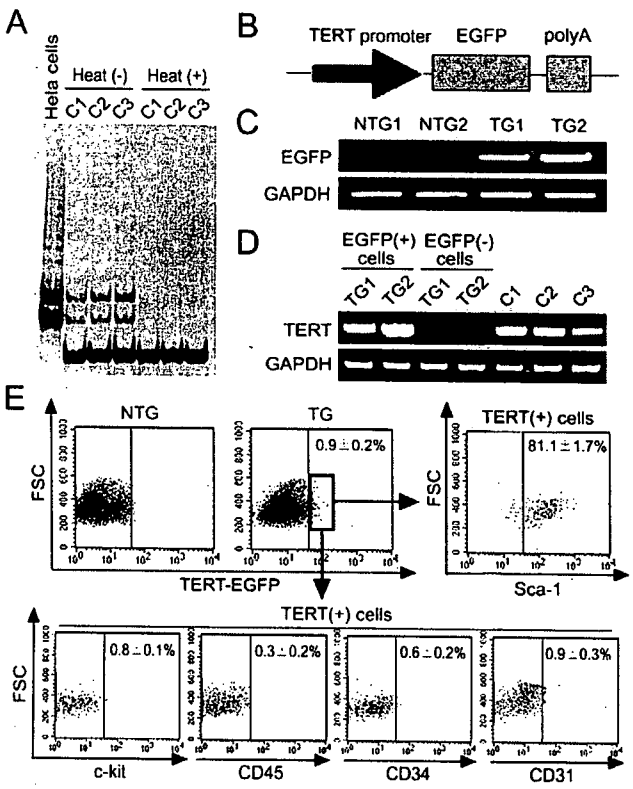

Fig. 2. TERT-expressing cells in adult heart are associated with Sca-1 expression. (A) Telomerase activity was measured by the TRAP assay in three independent clonal-CSCs. The cells were treated with or without heat and used as templates. Hela cells were used as positive controls. (B) Construction of EGFP transgene under the control of the TERT promoter. (C) PCR of genomic DNA from 2 independent TERT-EGFP transgenic lines and respective NTG littermate controls. (D) The expression of TERT on EGFP-positive and EGFP-negative cells sorted from TERT-EGFP transgenic hearts is shown by RT-PCR. The TERT expression was detectable in all three independent clonal CSCs shown in Fig. 1C. (E) FACS analysis of the primary EGFP-positive cells isolated from TERT-EGFP mice (TG). Expression of Sca-1, KIT, CD45, CD34, and CD31 in EGFP-positive cells was examined. Cells from NTG littermates were used as negative control. Data are representative of six independent experiments.

Generation of Sca-1 knockdown (KD) mice

To functionally characterize clonal CSCs, majority of which could be marked by Sca-1 expression, we generated Sca-1 KD mice in which double-stranded (ds)-Sca-1 RNA was expressed under the control of an RNA polymerase II promoter (Fig. 3A) (Shinagawa and Ishii, 2003). The vector pDECAP-Sca-1 expressing ds-Sca-1 RNA with a small loop for transcript pausing and full-length Sca-1 were co-transfected into HEK 293 cells at various concentrations, and the reduction in Sca-1 expression was examined by both RT-PCR and FACS (Fig. 3B,C). Two lines of Sca-1 KD mice were obtained, in which endogenous Sca-1 protein levels (Fig. 3D) in the heart were apparently reduced.

Targeting Sca-1 transcripts affects proliferation and survival but not differentiation of CSCs

To test the function of Sca-1 in CSC development, we examined the ability to clonally proliferate in vitro of single cells from the adult heart of Sca-1 KD and non-transgenic (NTG) littermate mice using a single-cell deposition analysis. This revealed that the percentage of colony-forming cells from Sca-1 KD hearts was significantly lower than that from NTG hearts (Sca-1 KD ~0.007% vs NTG ~0.03%, Fig. 3E). We isolated 11 clones from NTG hearts and four clones from Sca-1 KD hearts, of which eight NTG- and two Sca-1 KD-clones exhibited features of mesenchymal phenotype (data not shown), showed Nanog and Bcrp1 expression by RT-PCR, and could proliferate for more than 14 days (Fig. 3F). Of the clones obtained, four clones expressed brachyury, which is a primitive streak marker (Gadue et al., 2006). Sca-1 expression in CSCs isolated from Sca-1 KD mice was markedly inhibited compared with NTG controls (Fig. 3G). Therefore, we investigated whether Sca-1 expression affects the replicative growth of clonal CSCs in independent cell-culture (Fig. 3H). As shown in Fig. 3I, Sca-1 KD CSCs showed significantly impaired growth kinetics compared with those of NTG CSCs. We determined the molecular mechanisms by which Sca-1 KD mice showed retarded CSC growth. As shown in Fig. 3J, BrdU incorporation and phosphorylation of histone H3 were clearly reduced in the Sca-1 KD CSCs compared with NTG controls, whereas p53 expression levels were significantly increased in the Sca-1 KD CSCs. Telomerase activities were also significantly impaired in the Sca-1 KD CSCs (Fig. 3K).

Of the CSC clones isolated, clones 2, 3 and 6 from NTG and clone 1 from Sca-1 KD mice, all of which expressed brachyury, were chosen for subsequent series of experiments. We asked whether the decrease in clonal CSC growth mediated by Sca-1 KD is associated with an increase in apoptosis. CSCs were isolated from the hearts of NTG and Sca-1 KD mice and were incubated with 100 and 200 μM H_2O_2 for 18 hours, and the surviving cells were analyzed by TUNEL staining. As shown

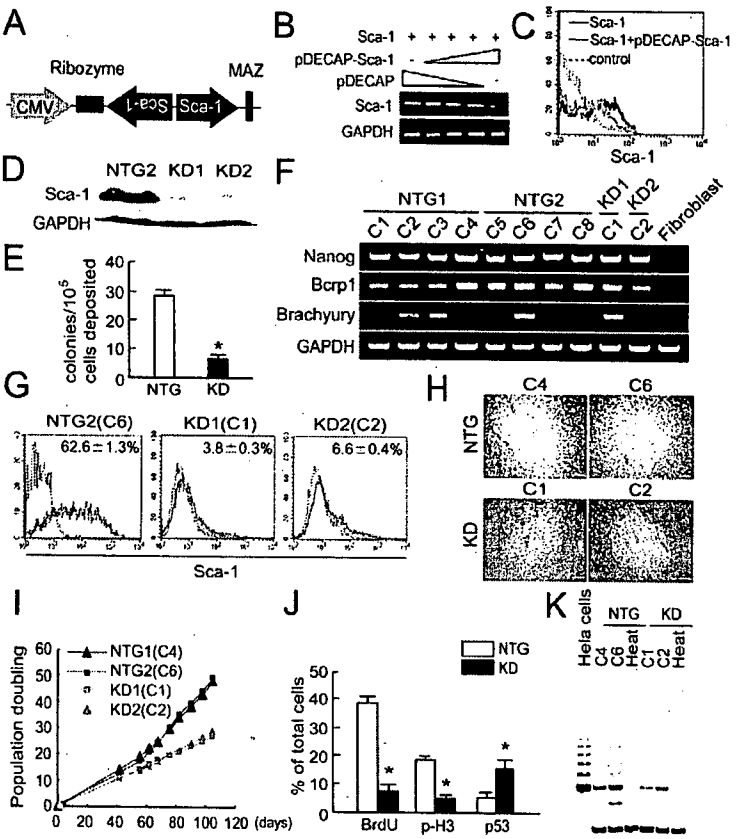

Fig. 3. Generation of Sca-1 KD mice. (A) Construction of the pDECAP-Sca-1 vector. (B,C) Decrease in exogenous Sca-1 expression induced by pDECAP-Sca-1 as shown by RT-PCR (B) and FACS (C) in HEK 293 cells. The total amount (8 μg) of plasmids co-transfected was the same in each experiment (n=3). (D) Decrease in Sca-1 protein levels in the hearts from two independent Sca-1 KD lines. (E) The frequency of CSC colonies from NTG- and Sca-1 KD hearts is shown. Data are expressed as the mean number of colonies formed per 10^5 single cells deposited ± s.e. (n=4). *P<0.01 vs NTG. (F) RT-PCR for embryonic and mesodermal precursor markers. Cardiac fibroblasts were used as negative control. (G) Decrease in Sca-1 expression from two independent Sca-1 KD CSCs clones. Black line, control IgG; red line, Sca-1. (H) Phase-contrast images of respective CSC clones at 14 days of culture in serum-free medium. Bars, 500 μm. (I) Growth kinetics of two independent clonal CSCs isolated from NTG (black lines, C4 and C6) and Sca-1 KD (red lines, C1 and C2) mice. (J) BrdU incorporation, phosphorylated histone-H3 (p-H3) and p53 expression from five independent experiments are shown. *P<0.01 vs NTG. (K) Loss of telomerase activity in the clonal CSCs (C1 and C2) isolated from two independent lines of Sca-1 KD mice.

in Fig. 4A, H_2O_2 induced apoptosis in a dose-dependent manner, and the extent of apoptosis was significantly higher in CSCs isolated from Sca-1 KD hearts than that in NTG-CSCs.

Activation of EGF and bFGF signaling in endothelial cells leads to the phosphorylation of a number of downstream effectors, including Akt and MAPKs (Sulpice et al., 2002). To test the role of these kinases in Sca-1-mediated CSC growth, the activation of Akt and MAPKs in response to EGF and bFGF was examined (Fig. 4B). Incubation of CSCs with EGF and bFGF resulted in a rapid enhancement of Akt, ERK1/2, and JNK1/2, but not in phosphorylation of p38. Although activation of Akt could be abolished by inhibition of Sca-1 transcripts, phosphorylation of three MAPKs was unaffected. These results raise the issue of whether Sca-1-mediated signaling regulates CSC differentiation in vitro. The potential of CSCs to give rise to cardiovascular lineages was not affected by targeting Sca-1 transcripts – as shown by immunostaining (Fig. 5A) and by RT-PCR to assess gene profiles typical of cardiac muscle, smooth muscle and endothelial cell differentiation after specific inductions for 14 days (Fig. 5B),

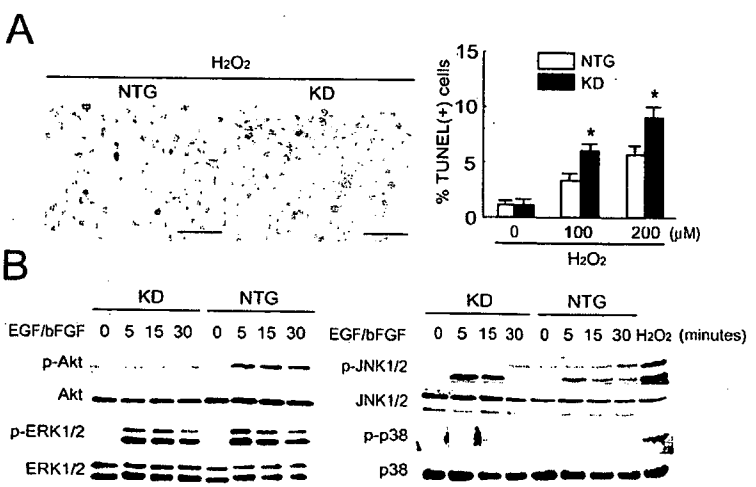

Fig. 4. Sca-1-mediated signaling activates Akt to support CSC proliferation and survival.
(A) Representative photographs of TUNEL assay obtained from NTG- or Sca-1 KD-derived CSCs treated with 200 μM H_2O_2 for 18 hours. The numbers of apoptotic cells (brown nuclei) in NTG (C6)- or Sca-1 KD-CSCs (C1) are shown (n=8). *P<0.01 versus NTG. (B) Loss of Sca-1 diminished EGF and bFGF-induced Akt activation in CSCs. CSCs treated with 200 μm H_2O_2 for 15 minutes were used as positive controls. Bars, 50 μm in A.

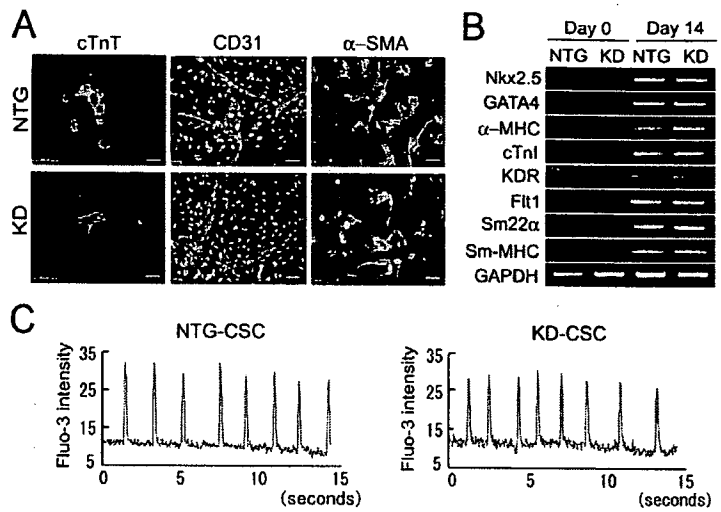

Fig. 5. Loss of Sca-1 transcripts does not affect the differentiation potential of clonal CSCs.
(A) Differentiation of NTG-derived or Sca-1 KD-derived clonal CSCs. Cardiac muscle cell (cardiac troponin-T), endothelial cell (CD31) and vascular smooth muscle cell (α-SMA) differentiation were 1.24±0.3%, 12.4±1.8% and 31.9±2.5%, respectively, for NTG-CSCs (C2, C3 and C6, respectively), and 1.23±0.3%, 12.1±2.1% and 32.2±4.7%, respectively, for Sca-1 KD-CSCs (C1). Nuclei are stained by DAPI (blue). Bars, 20 μm in A. (B) RT-PCR showed that the differentiation potential into the three different lineages were similar for both types of CSCs (n=3).
(C) Representative Ca^{2+} transient in beating cardiomyocytes. Clone 2, 3 and 6 from NTG and clone 1 from Sca-1 KD mice, all expressed brachyury at baseline, were used for analysis. Intensities were corrected by background amplitude and expressed as arbitrary units (n=3).

and a study investigating the Ca^{2+} transient in beating cardiomyocytes (Fig. 5C).

Loss of Sca-1 transcripts in CSCs fails to improve cardiac function due to diminished donor-cell proliferation, survival and engraftment after cell transplantation

The data described above support the hypothesis that loss of Sca-1 results in a retarded regenerative capacity of CSCs in vivo. To further examine this possibility, we performed cell transfer experiments into ischemic myocardium. 5×10^5 CSCs that had been clonally isolated and expanded from the hearts of Sca-1 KD (C1) and NTG (C6) mice were transplanted into wild-type (WT) mice 1 hour after myocardial infarction. Cardiac MRI was performed 4 weeks after cell grafting and showed that transplantation of Sca-1-KD CSCs resulted in significantly larger left ventricular volume and an increased infarct rate as compared with NTG-CSC implantation (Fig. 6A,B).

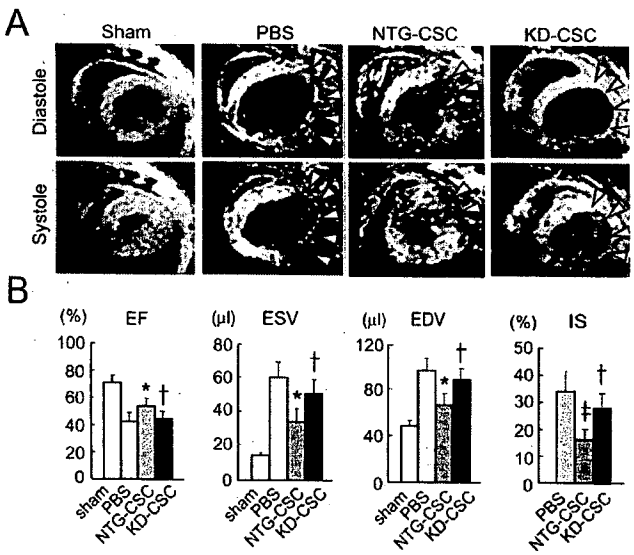

Fig. 6. Sca-1 KD CSC transplantation fails to prevent cardiac remodeling after myocardial infarction. (A,B) WT mice received transplantation of either NTG- or Sca-1 KD mice-derived CSCs 1 hour after infarction. Cardiac MRI was performed 4 weeks after CSC transplantation (n=8). Arrowheads indicate akinetic regions. White bars, sham-operated. Myocardial infarction with PBS injection (light gray bars), NTG-CSC (C6, dark gray bars) or Sca-1 KD-CSC (C1, black bars) transplantation are shown. *P<0.05 vs PBS; †P<0.05 versus NTG-CSC; ‡P<0.01 versus PBS injection. EF, ejection fraction; ESV, end-systolic volume; EDV, end-diastolic volume; IS, infarcted size.

We examined the in-vivo effects of Sca-1-mediated CSC regulation we observed in vitro. At day 3 after CSC transplantation into ischemic myocardium, Sca-1 KD CSCs showed significantly fewer engraftments than NTG-CSCs, as verified by measurement of *lacZ* activity (Fig. 7A). This observation was confirmed by the lower Ki67 expression in Sca-1 KD CSCs, indicating that the proliferative potential was significantly impaired in Sca-1 KD CSCs (Fig. 7A). To assess whether Sca-1-mediated control of CSC survival may also be applied to the process of donor-cell engraftment, we analyzed the viability of grafted CSCs, labeled by β-galactosidase (β-gal) staining, on day 3 after the cell grafting. As shown in Fig. 7B, grafted Sca-1 KD CSCs in the ischemic myocardium resulted in more apoptotic cells than NTG-CSCs, suggesting that the transplanted Sca-1 KD CSCs were also susceptible to cell death in vivo.

To further test whether these effects of Sca-1 during the early phase of CSC transplantation may contribute to the early CSC-engraftment and late regeneration process of cardiovascular-lineage cells, we investigated the presence of *lacZ*$^+$ donor cells at day 7 and characterized their individual phenotypes 4 weeks after transplantation. As shown in Fig. 8A, the frequency of *lacZ*$^+$ cells observed 7 days post cell transfer was significantly lower in Sca-1 KD CSC grafts compared with NTG-CSC transplantation, resulting in substantially insufficient cardiovascular regeneration within the ischemic regions 4 weeks after CSC transplantation (Fig. 8B-D).

Sca-1 KD CSC transplantation fails to prevent myocardial apoptosis and limits angiogenesis, partially due to the failure of paracrine effector secretion

Last, we assessed whether the loss of Sca-1 in transplanted

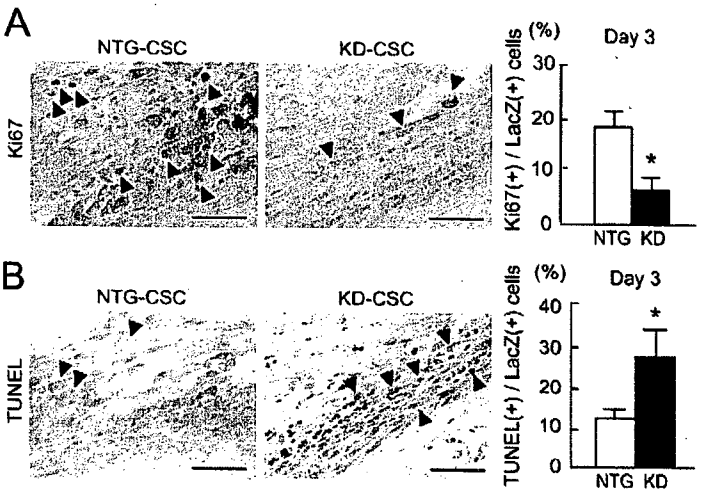

Fig. 7. Sca-1 transcripts are required for CSC proliferation and survival in vivo. (A) Immunohistochemistry of transplanted *lacZ*$^+$ cells 3 days after infarction. Transplanted *lacZ*$^+$ cells entering cell cycle were detected as Ki67-positive cells (arrowheads) (n=6). Myocardial infarction transplanted with NTG-CSCs (C6) and Sca-1 KD CSCs (C1) are shown. *P<0.01 versus NTG. (B) Apoptotic features (arrowheads, brown nuclei) of *lacZ*$^+$ engrafted cells are shown at day 3 after NTG- or Sca-1 KD-CSC transplantation. *P<0.01 versus NTG-CSC transplantation (n=6). Bars, 50 μm in A,B.

CSCs affects myocardial apoptosis and angiogenesis. At day 3, transplantation of Sca-1 KD CSCs resulted in a high level of myocardial apoptosis in the ungrafted area of the infarcted border zone, whereas fewer TUNEL-positive cells were observed in NTG-CSC-injected hearts (Fig. 9A). Furthermore, transplantation of Sca-1 KD CSCs failed to improve capillary density 2 weeks after infarction in the ischemic region as compared with NTG-CSC injection (Fig. 9B). To explore the molecular mechanisms of Sca-1-mediated myocardial apoptosis and neoangiogenesis, we then oxygen-starved CSCs for 8 hours and measured the levels of mRNA for secreted paracrine factors by RT-PCR. As shown in Fig. 9C, downregulation of hepatocyte growth factor (HGF) in Sca-1 KD CSCs was evident at baseline normoxia. After hypoxia, a greater increase in the expression of VEGF and HGF was observed in NTG-CSCs compared with that in Sca-1 KD CSCs. The expression pattern of insulin-like growth factor-1 (IGF1) under normoxic and hypoxic conditions was comparable in CSCs from NTG and Sca-1 KD hearts.

Discussion

Recent reports have shown that clonogenic CSCs reside in

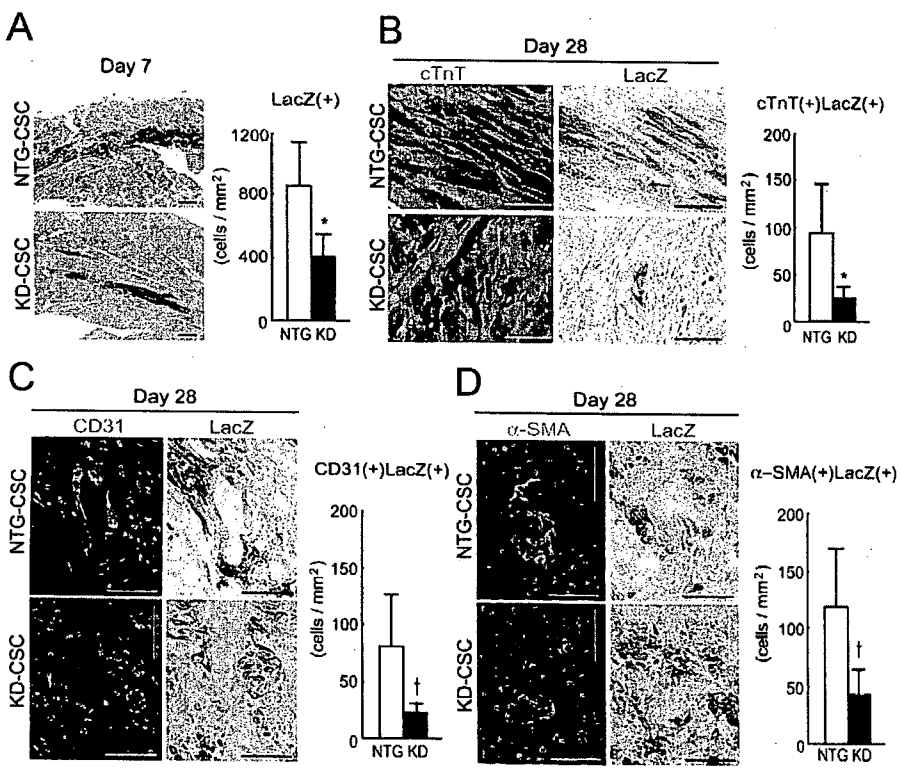

Fig. 8. Loss of Sca-1 transcripts in clonal CSC transplantation shows less donor-cell engraftment, resulting in the decrease in late cardiovascular regeneration. (A) Engrafted *lacZ*$^+$ cells in NTG (C6)- and Sca-1 KD-CSC (C1)-transplanted hearts at day 7 after infarction. Sections were counterstained using H&E. (B-D) The representative images and frequencies of cardiomyocytes (cardiac troponin-T, red), and endothelial (CD31) and smooth muscle cells (α-SMA) in *lacZ*$^+$ cells at day 28 are shown (n=6). Note that differentiated *lacZ*$^+$ cardiomyocytes co-express connexin-43 (yellow). Bars, 100 μm in A; 20 μm in B; 50 μm in C,D.

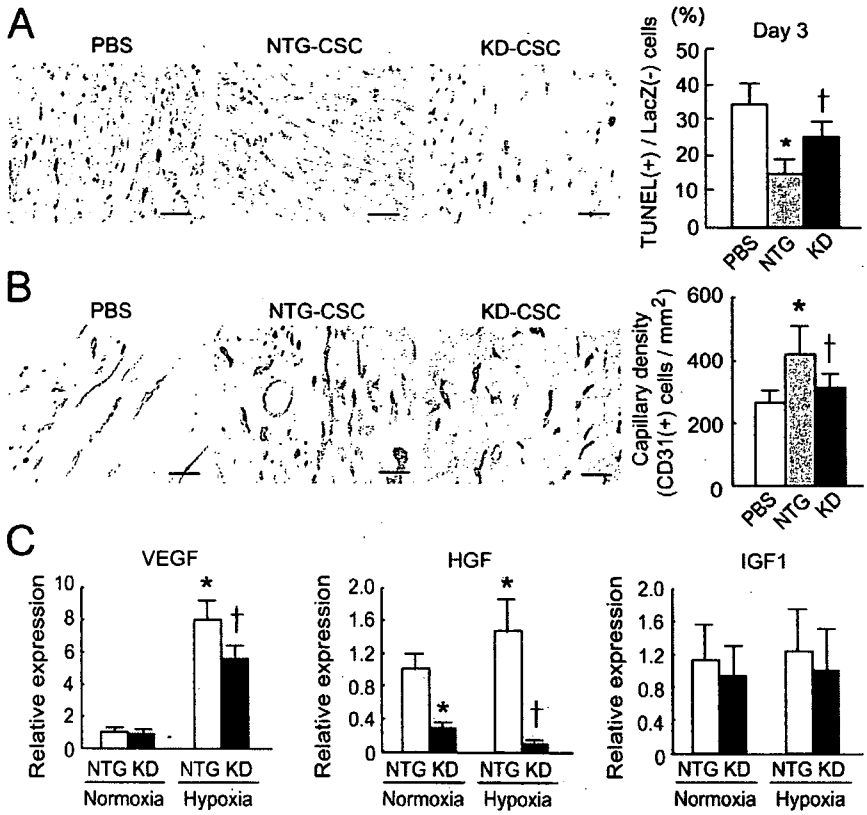

Fig. 9. Transplantation of Sca-1 KD CSCs fails to prevent myocardial apoptosis and limits neoangiogenesis after myocardial infarction partially due to the failure of paracrine effector secretion. (A) TUNEL staining revealed the apoptotic cardiomyocytes in the border zone of PBS-treated, NTG (C6)- and Sca-1 KD-CSC (C1)-transplanted hearts at day 3; (n=6). *P<0.01 vs PBS. †P<0.01 vs NTG. (B) Capillary density of infarcted border zone of transplanted hearts at day 14 after myocardial infarction. Capillary density was measured by staining of CD31 (brown) and corrected by the area analyzed. (n=8). *P<0.01 vs PBS-treated mice; †P<0.01 vs NTG-CSC-transplanted mice. Bars, 50 μm in A,B. (C) Relative mRNA expression levels of VEGF, HGF, and IGF1 normalized by 18S expression in NTG- and Sca-1 KD-CSCs under normoxic and hypoxic conditions (n=7). *P<0.01 vs NTG-CSCs under normoxia; †P<0.01 vs NTG-CSCs under hypoxia.

mammalian hearts, judging on the basis of specific cell-surface markers which are also expressed by hematopoietic and endothelial progenitor cells (Beltrami et al., 2003; Linke et al., 2005). Using an unbiased approach, our study has demonstrated that clonally proliferated CSCs express Sca-1 with ES cell-like and mesenchymal-cell-like characteristics, and are associated with TERT expression.

Our results, showing low expression of KIT in clonal *Kit*$^+$ CSCs, differ from the findings of some previous studies (Linke et al., 2005; Messina et al., 2004) but are consistent with those of recent reports about the adult heart (Fazel et al., 2006; Gude et al., 2006; Matsuura et al., 2004; Oh et al., 2003; Pfister et al., 2005; Tateishi et al., 2007). The reasons for this discrepancy are unclear. However, retrospective analysis data that directly sorted TERT-expressing cells from TERT-EGFP hearts (that were genetically isolated without the modification by cell culture) have shown that the majority of heart-resident TERT-positive cells could be identified via the expression of Sca-1. This implies that our findings were neither the result of intra-clonal variability nor due to contamination by cardiac fibroblasts during cell expansion. Recent report demonstrated that the expression levels of Sca-1 and KIT appear to be changed during myocardial maturation in ES cells (Wu et al., 2006).

Mesenchymal stem cells have been isolated from many tissues, including human heart (da Silva Meirelles et al., 2006; Tateishi et al., 2007). It is notable that CSCs expressed general characteristics of mesenchymal stem cells according to the analysis of cell-surface markers and partially showed the embryonic factors, as previously reported in clonal amniotic fluid-derived mesenchymal stem cells (Tsai et al., 2006). These observations indicated that the epithelial-mesenchymal transition (EMT) may occur in adult CSCs to produce proliferative precursors, which may undergo a reversible commitment into the directions of either mesenchymal or cardiac lineage, depending on the inductive conditions (Wessels and Perez-Pomares, 2004). Several reports suggest that the source of CSCs may include the neural crest (Tomita et al., 2005), primitive epicardial cells (Hay, 2005) or perivascular cells (da Silva Meirelles et al., 2006) through the EMT.

Regulating stem cell self-renewal is an essential feature of the niche where stem cells must be exposed to sufficient intrinsic-factors to maintain the proper stem cell number for the demands of tissue repair. We focused on Sca-1-mediated regulation in CSCs for the first time and found that normal Sca-1 function is associated with CSC proliferation and survival, contributing to early donor-cell engraftment and late cardiovascular differentiation, which is consistent with the prevailing view of the role of Sca-1 in the ability of hematopoietic stem cells and bone-marrow-derived mesenchymal stem cells to self-replicate (Bonyadi et al., 2003; Ito et al., 2003). Although the function of Sca-1 in skeletal muscle progenitors was not consistent with our observations in CSCs, the cell fate decision might be cell-type specific and/or age dependent (Mitchell et al., 2005). The mode of action of *Lin*$^-$*-Kit*$^+$ cells in the heart or bone marrow has been intensively investigated in gain- (Dawn et al., 2006; Urbanek et al., 2005a)

and loss-of-function experiments, and the function of these cells was validated by bone marrow reconstitution studies to completely rescue the defective cardiac repair in c-kit mutant mice after infarction (Ayach et al., 2006; Fazel et al., 2006), consistent with the lack of cardiac decompensation after pressure-overload in c-kit mutant mice (Hara et al., 2002) and our present observation indicating the rarity of c-kit$^+$ cells in TERT-expressing CSCs.

Sca-1 was originally identified as an antigen upregulated in activated lymphocytes, and was shown to be linked to the lipid bilayer as a glycosyl phosphatidylinositol (PtdIns)-anchored protein that activates cell signaling via mediators such as Akt (Reiser et al., 1986). The proliferation of CSCs appears to be dependent on the capacity of the cells to undergo cell cycle progression through the phosphorylation of Akt in response to EGF and bFGF stimulation, as observed in neural stem cells (Groszer et al., 2006). Our observations are supported by two independent gain-of-function studies demonstrating that the nuclear-targeting of Akt leads to the rapid expansion of comparatively rare *Kit*$^+$ CSCs in the postnatal heart (Gude et al., 2006), and ex-vivo transduction of Akt to bone marrow-derived MSCs can functionally repair the ischemic myocardium through the upregulation of secreted paracrine effectors (Gnecchi et al., 2006; Jiang et al., 2006). Consistent with these studies, our present study also demonstrated that the functional improvement of damaged myocardium after CSCs transplantation was attenuated by Sca-1 KD, in which new vessel formation and inhibition of myocardial apoptosis by release of angiogenic growth factors and myocyte regeneration by grafted CSCs were severely impaired.

Taken together, our results suggest that Sca-1 is expressed in the majority of intrinsic CSCs in the adult heart, which have characteristics of ES-like and mesenchymal-like cells, and implicate the role of Sca-1 in CSC maintenance and function. Sca-1-mediated signaling is important in CSC development in normal circumstances and its beneficial effect might be involved the responses to hypoxic and ischemic conditions. The cardioprotective effect of CSC transplantation that we have shown here indicates that Sca-1-mediated ligand responses may participate in the production of angiogenic and antiapoptotic paracrine effectors, consistent with recent observations demonstrating that induction of VEGF and HGF activates bone marrow-derived mesenchymal stem cells through PI 3-kinase–Akt pathway (Forte et al., 2006; Okuyama et al., 2006). It will be of interest to assess the gene expression profile in CSCs by targeting Sca-1 transcripts to identify the factors responsible for optimizing CSC therapy in heart failure.

Materials and Methods

Clonal isolation and culture of CSCs

Hearts from 6-week-old to-12-week-old GFP transgenic mice (provided by M. Okabe, Osaka University Medical School) (Okabe et al., 1997), Sca-1 KD mice or NTG mice were excised and were perfused with cold PBS to remove the blood cells. The tissues were washed twice, and aortic and pulmonary vessels were removed from the hearts. The dissected hearts were minced, and digested twice for 20 minutes at 37°C with 0.2% type II collagenase and 0.01% DNAse I (Worthington Biochemical Corp, NJ). The cells were passed through a 40-μm filter to remove the debris and were plated into 25-cm^2 dishes in DMEM (Invitrogen) for 30 minutes to allow fibroblasts to adhere. The non-adherent cells were collected and size-fractionated with a 30-70% Percoll gradient to obtain single-cell suspensions by removal of mature cardiomyocytes. For clonal analysis, the resulting cell suspensions were plated in 96-well plates at 1 cell per 100 μl by the limiting dilution technique (Yoon et al., 2005) with serum-free growth medium: DMEM/F12 containing B27 supplement, 20 ng/ml EGF (Sigma), and 40 ng/ml bFGF (Promega). Wells were visually inspected 24 hours after plating to exclude those containing more than one cell per well; then, clones derived from a single cell were further cultivated. On day 14, clonally expanded CSCs from single cells were cultured in low-serum medium consisting of growth medium supplemented with 1×B27 supplement, 2% FBS, and 10 ng/ml leukemia inhibitory factor (CHEMICON). At 60-70% confluence, cells from individual clones were serially reseeded in six-well plates, 25-cm^2, 75-cm^2 and 175-cm^2 flasks for further expansion. Hypoxic conditions were created by incubating cells at 37°C in a CO_2 multi-gas incubator (ASTEC) with an atmosphere of 5% CO_2 and 95% N_2 for 8 hours.

CSC differentiation

For cardiac differentiation analysis, single-cell-derived CSCs were cultured in differentiation medium containing 10% FBS, insulin-transferrin-selenium, and 10 nM dexamethasone (Sigma) for 14 days. Differentiation medium consisting of DMEM/F12 supplemented with 10 ng/ml VEGF or 50 ng/ml PDGF-BB (both from R&D Systems) and 10% FBS was used to induce endothelial and smooth muscle cell differentiation for 14 days, respectively.

Construction of targeting vector and generation of transgenic mice

Full-length Sca-1 cDNA was cloned using the following primers: forward: 5′-CTCTGAGGATGGACACTTCT-3′, reverse: 5′-GGTCTGCAGGAGGACTGA-GC-3′. The 404-bp ds-RNA fragment targeting the N-terminus of Sca-1 was selectively amplified and subcloned into the pDECAP vector (Shinagawa and Ishii, 2003). The plasmid encoding EGFP driven by the mouse *Tert* promoter was provided by N. Hole (University of Durham) (Armstrong et al., 2000) and subcloned into the human growth hormone polyadenylation sequence. Each expression cassette was released and microinjected into the pronuclei of fertilized C57BL/6 oocytes. PCR analysis of tail DNA was used to identify founder transgenic mice.

Retroviral transduction of CSCs

To track cells after injection into the infarcted myocardium, CSCs were engineered to express the bacterial *lacZ* reporter gene. This was done by retroviral infection with a vector (pMSCV-LacZ) encoding the *lacZ* gene and a puromycin resistance gene. After selection with puromycin, the transduction efficiency was evaluated by X-gal staining.

FACS analysis and cell sorting

Single-cell suspensions were stained with the following antibodies: phycoerythrin (PE)-conjugated antibodies against Sca-1, KIT, CD45, CD44, CD90, CD31, CD73, CD106, CD34, CD13, CD29, and isotype control IgG (all from BD Biosciences). Allophycocyanin (APC)-conjugated goat anti-rat IgG was used to detect rat anti-mouse CD105 (Southern Biotech). Dead cells were eliminated using propidium iodide (Sigma) and 10,000 to 50,000 events were collected per sample using a FACS Calibur flow cytometer (BD Biosciences). Bone marrow cells were flushed from the tibiae and femurs of 6-week-old to 12-week-old C57BL/6 mice and compared (with or without collagenase and filtration) (Oh et al., 2003). Single-cell suspensions were harvested from TERT-EGFP transgenic and NTG hearts as the method for CSC preparation, and the EGFP-positive cells were analyzed and sorted on BD FACSAria (Becton Dickinson).

RT-PCR and telomerase activity

Total RNA was prepared from cultured cells using TRIzol (Invitrogen) and cDNA was generated with the SuperScript III First-Strand Synthesis System (Invitrogen). PCR reactions were performed with gene-specific primers. Primer sequences are available on request. To evaluate VEGF, HGF, and IGF1 expression, cDNA was subjected to 40 rounds of amplification (ABI PRISM 7700, Applied Biosystems) with Assay-on-Demand™ primer-probes sets (Applied Biosystems). The mRNA levels were expressed relative to an endogenous control (18S RNA) and the fold-increase in the respective groups versus normoxia NTG-CSCs was calculated. Telomerase activity of single-cell-derived CSCs was measured using a TRAP assay kit, TRAPEZE (CHEMICON), as previously described (Oh et al., 2001).

Calcium transient

Cells were washed three times with 1 mM Ca^{2+} Tyrode's solution as previously described (Kaneko et al., 2000), additional 15 minutes incubation with 1 mM Ca^{2+} Tyrode's containing 1 mM probenecid at 37°C was performed to allow hydrolysis of acetoxymethyl esters within the cells. Fluorescence imaging was performed at 24°C using a fixed-stage microscope (BX50WI, Olympus, Japan) equipped with a multi-pinhole-type confocal scanning system (CSU-21, Yokogawa, Japan). Digitized fluorescence signals were analyzed with Image J software.

Western blotting

Whole protein lysates were extracted with lysis buffer: 50 mM Tris-HCl (pH 7.4), 150 mM NaCl, 0.25% sodium deoxycholate, 1 mM EDTA, 1% Nonidet P-40, 1 mM PMSF and protease inhibitor (PIERCE). For phosphorylation of Akt, ERK1/2, JNK1/2 and p38, 1 mM Na_3VO_4 and 1 mM NaF were added. Transferred

membranes were incubated with rat anti-mouse Sca-1 monoclonal antibody (clone D7, BD Biosciences), antibodies against phosphorylated Akt (S473), Akt, phosphorylated ERK1/2 (T202/Y204), ERK1/2, phosphorylated SAPK/JNK (Thr 183/Tyr185), SAPK/JNK, phosphorylated p38 MAPK (Thr180/Tyr182), p38 MAPK (all from Cell Signaling), or mouse monoclonal anti-GAPDH (Chemicon). Horseradish peroxidase (HRP)-conjugated goat anti-rat IgG, HRP-conjugated sheep anti-mouse IgG and HRP-conjugated donkey anti-rabbit IgG (Amersham Biosciences) were used as secondary antibodies.

Sample fixation and X-gal staining

Hearts were fixed in 1% paraformaldehyde, 0.2% glutaraldehyde, and 0.2% Nonidet P-40. X-gal staining was performed with the following reagents: 5 mM $K_4Fe(CN)_6$, 5 mM $K_3Fe(CN)_6$, 2 mM $MgCl_2$, 0.01% sodium deoxycholate, 0.2% Nonidet P-40, and 1 mg/ml X-gal (Invitrogen). After staining, samples were post-fixed with 4% paraformadehyde and embedded in frozen OCT compound or paraffin.

Histology and immunofluorescence

Fixed cells and frozen sections were stained using the following primary antibodies: mouse anti-cardiac troponin-T (Ab1, Neo Markers), rat anti-mouse CD31 (BD Biosciences), Cy3-conjugated anti-α-SMA (Sigma), rabbit anti-p53 (FL-393, Santa Cruz) and rabbit anti-phosphorylated histone H3 (Ser10, Upstate). Secondary antibodies were conjugated to Alexa Fluor 555 or Alexa Fluor 568, and nuclei were visualized using DAPI (Molecular Probes). BrdU incorporation was examined by incubation with 10 μM BrdU for 1 hour using a detection kit (Roche). For Ki67 immunohistochemistry, we used a Vectastain ABC Elite kit (Vector Laboratories). After antigen retrieval using citrate buffer (pH 6.0) and blockage of endogenous peroxidase activity using 0.3% hydrogen peroxide, the sections were incubated with rat anti-mouse Ki67 antibody (DAKO) for 1 hour at room temperature. Then, the sections were treated with biotinylated secondary antibody followed by incubation with avidin horseradish peroxidase complex. Finally, the sections were counterstained with hematoxylin or H&E staining. Capillary density was estimated by CD31 immunostaining with a Vectastain ABC Elite kit. Apoptotic CSCs or cardiomyocytes were evaluated by the TUNEL assay in fixed cells and paraffin-embedded sections with an ApopTag kit (Chemicon). H_2O_2 was purchased from Wako. Images were captured with a BZ-8000 (Keyence, Japan) and IX 71 (Olympus Corporation, Japan).

Myocardial infarction and cell grafting

Ligation of the left anterior descending (LAD) coronary artery was performed in 12-week-old to 24-week-old C57BL/6 mice (Shimizu Laboratory Supplies, Japan) in accordance with the animal care and use guidelines at Kyoto University Hospital. One hour after the LAD ligation, 5×10^5 cells were suspended in 20 μl of PBS and injected into two sites of the infarcted border zone. In the control group, mice were sham-operated by receiving a left thoracotomy without coronary artery ligation.

Cardiac function and infarct size

Cardiac MRI studies were performed using a 7 T MR scanner, Unity Inova (Varian Inc., Palo Alto, CA) with a 25-mm home-built solenoid-type volume coil. Analysis of end-systolic and end-diastolic LV volumes and LV mass was done using an operator-interactive threshold technique, and stroke volume and cardiac output were calculated. All measurements were performed and analyzed by an individual blinded to the animal group. For in vivo determination of infarct size, end-diastolic epicardial and endocardial contours were traced on the MRI short-axis slices; only akinetic and dyskinetic segments were considered to be infarcted areas (Yang et al., 2004).

Statistics

Data are expressed as the mean ± s.e. Two-tailed Student's *t* test was used to compare the clonality of Sca-1 KD- and NTG-CSCs. Comparison of groups in remaining experiments was unpaired analyses using two-tailed Student's *t* test. Significance level was set at $P<0.05$ (StatView).

We thank the following investigators for their kind gifts of mice or plasmids: M. Okabe, N. Hole, S. Ishii and Y. Yoshida, A. Kosugi. We also thank M. Nishikawa for technical assistance. This work was supported by Grants-in-Aid from the Ministry of Education, Culture, Sports, Science and Technology, and by Grants-in-Aid from the Ministry of Health, Labor and Welfare.

References

Armstrong, L., Lako, M., Lincoln, J., Cairns, P. M. and Hole, N. (2000). mTert expression correlates with telomerase activity during the differentiation of murine embryonic stem cells. *Mech. Dev.* **97**, 109-116.

Ayach, B. B., Yoshimitsu, M., Dawood, F., Sun, M., Arab, S., Chen, M., Higuchi, K., Siatskas, C., Lee, P., Lim, H. et al. (2006). Stem cell factor receptor induces progenitor and natural killer cell-mediated cardiac survival and repair after myocardial infarction. *Proc. Natl. Acad. Sci. USA* **103**, 2304-2309.

Beltrami, A. P., Barlucchi, L., Torella, D., Baker, M., Limana, F., Chimenti, S., Kasahara, H., Rota, M., Musso, E., Urbanek, K. et al. (2003). Adult cardiac stem cells are multipotent and support myocardial regeneration. *Cell* **114**, 763-776.

Blackburn, E. H. (2001). Switching and signaling at the telomere. *Cell* **106**, 661-673.

Bonyadi, M., Waldman, S. D., Liu, D., Aubin, J. E., Grynpas, M. D. and Stanford, W. L. (2003). Mesenchymal progenitor self-renewal deficiency leads to age-dependent osteoporosis in Sca-1/Ly-6A null mice. *Proc. Natl. Acad. Sci. USA* **100**, 5840-5845.

da Silva Meirelles, L., Chagastelles, P. C. and Nardi, N. B. (2006). Mesenchymal stem cells reside in virtually all post-natal organs and tissues. *J. Cell Sci.* **119**, 2204-2213.

Dawn, B., Guo, Y., Rezazadeh, A., Huang, Y., Stein, A. B., Hunt, G., Tiwari, S., Varma, J., Gu, Y., Prabhu, S. D. et al. (2006). Postinfarct cytokine therapy regenerates cardiac tissue and improves left ventricular function. *Circ. Res.* **98**, 1098-1105.

Fazel, S., Cimini, M., Chen, L., Li, S., Angoulvant, D., Fedak, P., Verma, S., Weisel, R. D., Keating, A. and Li, R. K. (2006). Cardioprotective c-kit+ cells are from the bone marrow and regulate the myocardial balance of angiogenic cytokines. *J. Clin. Invest.* **116**, 1865-1877.

Forte, G., Minieri, M., Cossa, P., Antenucci, D., Sala, M., Gnocchi, V., Fiaccavento, R., Carotenuto, F., De Vito, P., Baldini, P. M. et al. (2006). Hepatocyte growth factor effects on mesenchymal stem cells: proliferation, migration, and differentiation. *Stem Cells* **24**, 23-33.

Gadue, P., Huber, T. L., Paddison, P. J. and Keller, G. M. (2006). Wnt and TGF-beta signaling are required for the induction of an in vitro model of primitive streak formation using embryonic stem cells. *Proc. Natl. Acad. Sci. USA* **103**, 16806-16811.

Gnecchi, M., He, H., Noiseux, N., Liang, O. D., Zhang, L., Morello, F., Mu, H., Melo, L. G., Pratt, R. E., Ingwall, J. S. et al. (2006). Evidence supporting paracrine hypothesis for Akt-modified mesenchymal stem cell-mediated cardiac protection and functional improvement. *FASEB J.* **20**, 661-669.

Groszer, M., Erickson, R., Scripture-Adams, D. D., Dougherty, J. D., Le Belle, J., Zack, J. A., Geschwind, D. H., Liu, X., Kornblum, H. I. and Wu, H. (2006). PTEN negatively regulates neural stem cell self-renewal by modulating G0-G1 cell cycle entry. *Proc. Natl. Acad. Sci. USA* **103**, 111-116.

Gude, N., Muraski, J., Rubio, M., Kajstura, J., Schaefer, E., Anversa, P. and Sussman, M. A. (2006). Akt promotes increased cardiomyocyte cycling and expansion of the cardiac progenitor cell population. *Circ. Res.* **99**, 381-388.

Hara, M., Ono, K., Hwang, M. W., Iwasaki, A., Okada, M., Nakatani, K., Sasayama, S. and Matsumori, A. (2002). Evidence for a role of mast cells in the evolution to congestive heart failure. *J. Exp. Med.* **195**, 375-381.

Hay, E. D. (2005). The mesenchymal cell, its role in the embryo, and the remarkable signaling mechanisms that create it. *Dev. Dyn.* **233**, 706-720.

Ito, C. Y., Li, C. Y., Bernstein, A., Dick, J. E. and Stanford, W. L. (2003). Hematopoietic stem cell and progenitor defects in Sca-1/Ly-6A-null mice. *Blood* **101**, 517-523.

Jiang, S., Haider, H., Idris, N. M., Salim, A. and Ashraf, M. (2006). Supportive interaction between cell survival signaling and angiocompetent factors enhances donor cell survival and promotes angiomyogenesis for cardiac repair. *Circ. Res.* **99**, 776-784.

Joannides, A., Gaughwin, P., Schwiening, C., Majed, H., Sterling, J., Compston, A. and Chandran, S. (2004). Efficient generation of neural precursors from adult human skin: astrocytes promote neurogenesis from skin-derived stem cells. *Lancet* **364**, 172-178.

Kaneko, T., Tanaka, H., Oyamada, M., Kawata, S. and Takamatsu, T. (2000). Three distinct types of Ca(2+) waves in Langendorff-perfused rat heart revealed by real-time confocal microscopy. *Circ. Res.* **86**, 1093-1099.

Kawada, H., Fujita, J., Kinjo, K., Matsuzaki, Y., Tsuma, M., Miyatake, H., Muguruma, Y., Tsuboi, K., Itabashi, Y., Ikeda, Y. et al. (2004). Nonhematopoietic mesenchymal stem cells can be mobilized and differentiate into cardiomyocytes after myocardial infarction. *Blood* **104**, 3581-3587.

Laugwitz, K. L., Moretti, A., Lam, J., Gruber, P., Chen, Y., Woodard, S., Lin, L. Z., Cai, C. L., Lu, M. M., Reth, M. et al. (2005). Postnatal isl1+ cardioblasts enter fully differentiated cardiomyocyte lineages. *Nature* **433**, 647-653.

Leri, A., Barlucchi, L., Limana, F., Deptala, A., Darzynkiewicz, Z., Hintze, T. H., Kajstura, J., Nadal-Ginard, B. and Anversa, P. (2001). Telomerase expression and activity are coupled with myocyte proliferation and preservation of telomeric length in the failing heart. *Proc. Natl. Acad. Sci. USA* **98**, 8626-8631.

Limana, F., Germani, A., Zacheo, A., Kajstura, J., Di Carlo, A., Borsellino, G., Leoni, O., Palumbo, R., Battistini, L., Rastaldo, R. et al. (2005). Exogenous high-mobility group box 1 protein induces myocardial regeneration after infarction via enhanced cardiac C-kit+ cell proliferation and differentiation. *Circ. Res.* **97**, e73-e83.

Linke, A., Muller, P., Nurzynska, D., Casarsa, C., Torella, D., Nascimbene, A., Castaldo, C., Cascapera, S., Bohm, M., Quaini, F. et al. (2005). Stem cells in the dog heart are self-renewing, clonogenic, and multipotent and regenerate infarcted myocardium, improving cardiac function. *Proc. Natl. Acad. Sci. USA* **102**, 8966-8971.

Matsuura, K., Nagai, T., Nishigaki, N., Oyama, T., Nishi, J., Wada, H., Sano, M., Toko, H., Akazawa, H., Sato, T. et al. (2004). Adult cardiac Sca-1-positive cells differentiate into beating cardiomyocytes. *J. Biol. Chem.* **279**, 11384-11391.

Messina, E., De Angelis, L., Frati, G., Morrone, S., Chimenti, S., Fiordaliso, F., Salio, M., Battaglia, M., Latronico, M. V., Coletta, M. et al. (2004). Isolation and expansion of adult cardiac stem cells from human and murine heart. *Circ. Res.* **95**, 911-921.

Mitchell, P. O., Mills, T., O'Connor, R. S., Graubert, T., Dzierzak, E. and Pavlath, G. K. (2005). Sca-1 negatively regulates proliferation and differentiation of muscle cells. *Dev. Biol.* **283**, 240-252.

Moretti, A., Caron, L., Nakano, A., Lam, J. T., Bernshausen, A., Chen, Y., Qyang, Y., Bu, L., Sasaki, M., Martin-Puig, S. et al. (2006). Multipotent embryonic Isl1(+)

progenitor cells lead to cardiac, smooth muscle, and endothelial cell diversification. *Cell* **127**, 1151-1165.

Murry, C. E., Soonpaa, M. H., Reinecke, H., Nakajima, H., Nakajima, H. O., Rubart, M., Pasumarthi, K. B., Virag, J. I., Bartelmez, S. H., Poppa, V. et al. (2004). Haematopoietic stem cells do not transdifferentiate into cardiac myocytes in myocardial infarcts. *Nature* **428**, 664-668.

Oh, H., Taffet, G. E., Youker, K. A., Entman, M. L., Overbeek, P. A., Michael, L. H. and Schneider, M. D. (2001). Telomerase reverse transcriptase promotes cardiac muscle cell proliferation, hypertrophy, and survival. *Proc. Natl. Acad. Sci. USA* **98**, 10308-10313.

Oh, H., Bradfute, S. B., Gallardo, T. D., Nakamura, T., Gaussin, V., Mishina, Y., Pocius, J., Michael, L. H., Behringer, R. R., Garry, D. J. et al. (2003). Cardiac progenitor cells from adult myocardium: homing, differentiation, and fusion after infarction. *Proc. Natl. Acad. Sci. USA* **100**, 12313-12318.

Okabe, M., Ikawa, M., Kominami, K., Nakanishi, T. and Nishimune, Y. (1997). 'Green mice' as a source of ubiquitous green cells. *FEBS Lett.* **407**, 313-319.

Okuyama, H., Krishnamachary, B., Zhou, Y. F., Nagasawa, H., Bosch-Marce, M. and Semenza, G. L. (2006). Expression of vascular endothelial growth factor receptor 1 in bone marrow-derived mesenchymal cells is dependent on hypoxia-inducible factor 1. *J. Biol. Chem.* **281**, 15554-15563.

Orlic, D., Kajstura, J., Chimenti, S., Jakoniuk, I., Anderson, S. M., Li, B., Pickel, J., McKay, R., Nadal-Ginard, B., Bodine, D. M. et al. (2001). Bone marrow cells regenerate infarcted myocardium. *Nature* **410**, 701-705.

Pfister, O., Mouquet, F., Jain, M., Summer, R., Helmes, M., Fine, A., Colucci, W. S. and Liao, R. (2005). CD31- but not CD31+ cardiac side population cells exhibit functional cardiomyogenic differentiation. *Circ. Res.* **97**, 52-61.

Pittenger, M. F. and Martin, B. J. (2004). Mesenchymal stem cells and their potential as cardiac therapeutics. *Circ. Res.* **95**, 9-20.

Reiser, H., Oettgen, H., Yeh, E. T., Terhorst, C., Low, M. G., Benacerraf, B. and Rock, K. L. (1986). Structural characterization of the TAP molecule: a phosphatidylinositol-linked glycoprotein distinct from the T cell receptor/T3 complex and Thy-1. *Cell* **47**, 365-370.

Rota, M., LeCapitaine, N., Hosoda, T., Boni, A., De Angelis, A., Padin-Iruegas, M. E., Esposito, G., Vitale, S., Urbanek, K., Casarsa, C. et al. (2006). Diabetes promotes cardiac stem cell aging and heart failure, which are prevented by deletion of the p66shc gene. *Circ. Res.* **99**, 42-52.

Shinagawa, T. and Ishii, S. (2003). Generation of Ski-knockdown mice by expressing a long double-strand RNA from an RNA polymerase II promoter. *Genes Dev.* **17**, 1340-1345.

Sulpice, E., Bryckaert, M., Lacour, J., Contreres, J. O. and Tobelem, G. (2002). Platelet factor 4 inhibits FGF2-induced endothelial cell proliferation via the extracellular signal-regulated kinase pathway but not by the phosphatidylinositol 3-kinase pathway. *Blood* **100**, 3087-3094.

Takahashi, K. and Yamanaka, S. (2006). Induction of pluripotent stem cells from mouse embryonic and adult fibroblast cultures by defined factors. *Cell* **126**, 663-676.

Tateishi, K., Ashihara, E., Honsho, S., Takehara, N., Nomura, T., Takahashi, T., Ueyama, T., Yamagishi, M., Yaku, H., Matsubara, H. et al. (2007). Human cardiac stem cells exhibit mesenchymal features and are maintained through Akt/GSK-3beta signaling. *Biochem. Biophys. Res. Commun.* **352**, 635-641.

Tomita, Y., Matsumura, K., Wakamatsu, Y., Matsuzaki, Y., Shibuya, I., Kawaguchi, H., Ieda, M., Kanakubo, S., Shimazaki, T., Ogawa, S. et al. (2005). Cardiac neural crest cells contribute to the dormant multipotent stem cell in the mammalian heart. *J. Cell Biol.* **170**, 1135-1146.

Tsai, M. S., Hwang, S. M., Tsai, Y. L., Cheng, F. C., Lee, J. L. and Chang, Y. J. (2006). Clonal amniotic fluid-derived stem cells express characteristics of both mesenchymal and neural stem cells. *Biol. Reprod.* **74**, 545-551.

Urbanek, K., Quaini, F., Tasca, G., Torella, D., Castaldo, C., Nadal-Ginard, B., Leri, A., Kajstura, J., Quaini, E. and Anversa, P. (2003). Intense myocyte formation from cardiac stem cells in human cardiac hypertrophy. *Proc. Natl. Acad. Sci. USA* **100**, 10440-10445.

Urbanek, K., Rota, M., Cascapera, S., Bearzi, C., Nascimbene, A., De Angelis, A., Hosoda, T., Chimenti, S., Baker, M., Limana, F. et al. (2005a). Cardiac stem cells possess growth factor-receptor systems that after activation regenerate the infarcted myocardium, improving ventricular function and long-term survival. *Circ. Res.* **97**, 663-673.

Urbanek, K., Torella, D., Sheikh, F., De Angelis, A., Nurzynska, D., Silvestri, F., Beltrami, C. A., Bussani, R., Beltrami, A. P., Quaini, F. et al. (2005b). Myocardial regeneration by activation of multipotent cardiac stem cells in ischemic heart failure. *Proc. Natl. Acad. Sci. USA* **102**, 8692-8697.

Urbanek, K., Cesselli, D., Rota, M., Nascimbene, A., De Angelis, A., Hosoda, T., Bearzi, C., Boni, A., Bolli, R., Kajstura, J. et al. (2006). Stem cell niches in the adult mouse heart. *Proc. Natl. Acad. Sci. USA* **103**, 9226-9231.

Wessels, A. and Perez-Pomares, J. M. (2004). The epicardium and epicardially derived cells (EPDCs) as cardiac stem cells. *Anat. Rec. A Discov. Mol. Cell. Evol. Biol.* **276**, 43-57.

Wu, S. M., Fujiwara, Y., Cibulsky, S. M., Clapham, D. E., Lien, C. L., Schultheiss, T. M. and Orkin, S. H. (2006). Developmental origin of a bipotential myocardial and smooth muscle cell precursor in the Mammalian heart. *Cell* **127**, 1137-1150.

Yang, Z., Berr, S. S., Gilson, W. D., Toufektsian, M. C. and French, B. A. (2004). Simultaneous evaluation of infarct size and cardiac function in intact mice by contrast-enhanced cardiac magnetic resonance imaging reveals contractile dysfunction in noninfarcted regions early after myocardial infarction. *Circulation* **109**, 1161-1167.

Yoon, Y. S., Wecker, A., Heyd, L., Park, J. S., Tkebuchava, T., Kusano, K., Hanley, A., Scadova, H., Qin, G., Cha, D. H. et al. (2005). Clonally expanded novel multipotent stem cells from human bone marrow regenerate myocardium after myocardial infarction. *J. Clin. Invest.* **115**, 326-338.

Available online at www.sciencedirect.com
ScienceDirect
Biochemical and Biophysical Research Communications 352 (2007) 635–641
BBRC
www.elsevier.com/locate/ybbrc

Human cardiac stem cells exhibit mesenchymal features and are maintained through Akt/GSK-3β signaling

Kento Tateishi [a,b], Eishi Ashihara [a], Shoken Honsho [a,b], Naofumi Takehara [a], Tetsuya Nomura [a,b], Tomosaburo Takahashi [b], Tomomi Ueyama [a], Masaaki Yamagishi [c], Hitoshi Yaku [c], Hiroaki Matsubara [a,b,*], Hidemasa Oh [a,*]

[a] *Department of Experimental Therapeutics, Translational Research Center, Kyoto University Hospital, Kyoto 606-8507, Japan*
[b] *Department of Cardiovascular Medicine, Kyoto Prefectural University School of Medicine, Kyoto 602-8566, Japan*
[c] *Department of Cardiovascular Surgery, Kyoto Prefectural University School of Medicine, Kyoto 602-8566, Japan*

Received 9 November 2006
Available online 27 November 2006

Abstract

Recent evidence suggested that human cardiac stem cells (hCSCs) may have the clinical application for cardiac repair; however, their characteristics and the regulatory mechanisms of their growth have not been fully investigated. Here, we show the novel property of hCSCs with respect to their origin and tissue distribution in human heart, and demonstrate the signaling pathway that regulates their growth and survival. Telomerase-active hCSCs were predominantly present in the right atrium and outflow tract of the heart (infant > adult) and had a mesenchymal cell-like phenotype. These hCSCs expressed the embryonic stem cell markers and differentiated into cardiomyocytes to support cardiac function when transplanted them into ischemic myocardium. Inhibition of Akt pathway impaired the hCSC proliferation and induced apoptosis, whereas inhibition of glycogen synthase kinase-3 (GSK-3) enhanced their growth and survival. We conclude that hCSCs exhibit mesenchymal features and that Akt/GSK-3β may be crucial modulators for hCSC maintenance in human heart.

Keywords: Cardiac stem cells; Mesenchymal cells; Proliferation; Survival; Akt/GSK-3β

The postmitotic heart was shown to exhibit a previously unappreciated self-renewing phenotype, in which primitive cells proliferated and differentiated into specific progeny under acute or chronic workloads [1,2]. Recent studies have challenged this paradigm and shown the existence of intrinsic cardiac stem or progenitor cells in the mammalian heart [3–5]. CSCs expressing c-kit were clonogenic and multipotent [4,6], and were also able to be isolated from human heart in the floating culture system [7]. Furthermore, hCSCs were reported to be activated in response to myocardial ischemia and increased workload [8,9]. These cells have a significant impact on future clinical application to treat patients with heart failure. However, it is necessary to further examine the property and regulatory mechanism of hCSC growth to obtain a sufficient number of stem cells from a small amount of tissue samples to achieve an efficient regenerative-therapy.

Recent reports have suggested that bone marrow-derived mesenchymal stem cells (MSCs) enhanced with Akt, a serine/threonine protein kinase, can repair infarcted myocardium, prevent remodeling, and normalize cardiac performance through the prevention of apoptosis as well as a paracrine effect on resident cells [10,11]. Recently, insulin-like growth factor-1 (IGF1) has been shown to maintain murine CSC (mCSC) viability and growth through activation of Akt [12,13]; however, the downstream signals of

* Corresponding authors. Fax: +81 75 751 4741.
E-mail addresses: matsubah@koto.kpu-m.ac.jp (H. Matsubara), hidemasa@kuhp.kyoto-u.ac.jp (H. Oh).

0006-291X/$ - see front matter © 2006 Elsevier Inc. All rights reserved.
doi:10.1016/j.bbrc.2006.11.096

Akt pathway in hCSC growth remain to be investigated. In the present study, we characterized the property of hCSCs and clarified the role of Akt/GSK-3β signaling pathway in hCSC growth and survival. These results suggest that pharmacological inhibition of GSK-3β may have practical application in hCSC transplantation therapy in human heart failure.

Materials and methods

Tissue samples. The heart samples were obtained from 18 patients undergone cardiac surgery (9 males and 9 females aged from 9 days to 77 years old) in confirmation with the guidelines of the Kyoto University Hospital and Ministry of Education, Culture, Sports, Science, and Technology, Japan.

Isolation of hCSCs. The heart samples were excised, minced, and digested with 0.4% type II collagenase and 0.01% DNAse. Obtained cells were then plated at 20 cells/μl in ultra-low culture dishes to generate cardiospheres with growth medium containing DMEM/F12, 5% FBS, 20 ng/ml EGF (Sigma), and 40 ng/ml bFGF (Promega). For the analyses described below, generated cardiospheres were dissected into single cells to obtain hCSCs by exposure to a 0.05% Trypsin/EDTA solution.

hCSC differentiation. For cardiac differentiation, hCSCs were cultured in differentiation medium containing 10% FBS, insulin-transferrin-selenium, and 10 nM dexamethasone. Differentiation medium containing DMEM/F12 supplemented with 10 ng/ml VEGF or 50 ng/ml PDGF-BB (R&D Systems) and 10% FBS was used to induce endothelial or smooth muscle cell differentiation, respectively. For the assay of cell proliferation and survival, specific inhibitors for Akt and GSK-3 (BIO) were purchased from Calbiochem.

FACS analysis. hCSCs were labeled with the following antibodies; phycoerythrin-conjugated antibodies against c-kit, CD45, CD34, CD31, CD90, CD29, CD73, CD71 (BD Biosciences), CD105 (Ancell Corp), and Stro-1 (R&D Systems). Cell events were collected by FACS Calibur flow cytometer and data were analyzed by Cell Quest (BD Biosciences).

RT-PCR and telomerase activity. Total RNA was extracted from cells using TRIzol and RT-PCR was performed with a SuperScript III First-Strand Synthesis System. The primer sequences are available upon request. Telomerase activity was measured with a TRAP assay kit, TRAPEZE (Chemicon).

Immunochemistry. Fixed cells and sections were stained with primary antibodies against cardiac troponin-I (Scripps), CD31, Ki67 (DAKO), α-SMA, connexin 43 (Sigma), collagen typeI (LSL), vimentin, and human nuclei (Chemicon). Secondary antibodies were conjugated to Alexa 488 and Alexa 555, and nuclei were visualized with 4′,6-diamidino-2-phenylindole (DAPI). Apoptotic hCSCs were evaluated by TUNEL assay with ApopTag kit (Chemicon). Images were captured with a BZ-8000 (Keyence) and IX71 (Olympus Corporation).

Myocardial infarction (MI) and cell grafting. MI was created in 12- to 24-week-old NOD/*scid* mice (Jackson Laboratories) in accordance with the animal care and use guidelines at Kyoto University Hospital. MI was induced by ligation of the left anterior descending coronary artery. One hour after MI, 3×10^5 hCSCs were injected into two sites of the infarcted border zone. In the control group, mice were sham-operated on receiving a thoracotomy but no ligation of coronary artery.

Echocardiography. Two-dimensional and M-mode recordings (Sonos 5500, PHILIPS) were obtained from the short-axis view at the midpapillary muscle level.

Western blotting. Cell lysates were extracted with lysis buffer containing 50 mM Tris–HCl (pH 7.4), 150 mM NaCl, 0.25% sodium deoxycholate, 1 mM EDTA, 1% Nonidet P-40, 1 mM PMSF, 1× protease inhibitor, 1 mM Na_3VO_4, and 1 mM NaF. Transferred membranes were incubated with primary antibodies against GSK-3β (BD Biosciences), phospho-GSK-3β (Ser9), phospho-Akt (S473), and Akt (Cell Signaling). Horseradish peroxidase (HRP)-conjugated anti-mouse IgG and HRP-conjugated anti-rabbit IgG were used as secondary antibodies.

Statistics. Data are means ± SE, and were analyzed by ANOVA and Scheffe's test, using a significance level of $p < 0.05$ (StatView).

Results

Identification and distribution of hCSCs in human heart

To characterize the hCSCs in human heart, primary heart-derived cells from patients were cultured at low density with low serum condition in a floating culture system using a modification of the method previously reported [7]. At day-14, spherical colonies were generated at a frequency of 63.1 ± 16.5 spheres per 200,000 viable cells (Fig. 1A). The initial yield of digested cells was proportional to the number of spheres, and the number of isolated cells was significantly increased in heart tissues from the right atrium (RA) and outflow tract (OFT) than in tissue from the left ventricle (LV) (Fig. 1B). Moreover, the isolated cells were 5-fold greater and had higher telomerase activity in the infant heart than the adult heart (Fig. 1C and D).

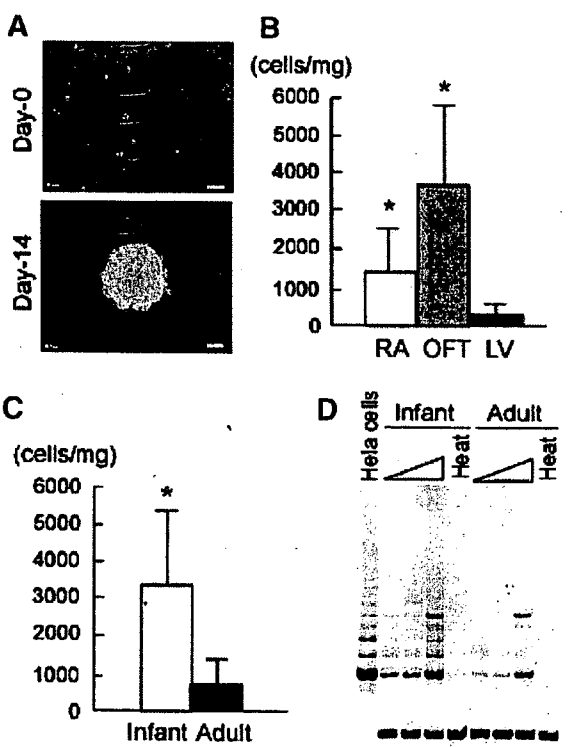

Fig. 1. Isolation and distribution of hCSCs. (A) Generation of cardiosphere from human heart. Bars, 20 μm. (B, C) The initial progenitor cell number harvested by primary isolation as indicated. Total yield was corrected by tissue weight (mg). Distribution of hCSCs corresponding to the parts of the heart (B) or the patients' age (C). $^*p < 0.05$ versus LV in (B); $^*p < 0.01$ versus adult in (C). (D) Telomerase activity in hCSCs. Threefold serial dilutions of hCSCs isolated from infant and adult hearts were treated with or without heat and used as templates. HeLa cells were used as a positive control ($n = 3$).

hCSCs exhibit mesenchymal features

Immunophenotyping revealed that hCSCs rarely expressed c-kit and did not express the hematopoietic and endothelial progenitor cell-specific surface antigens: CD45, CD34, and CD31, while they were positive for typical MSC surface antigens: CD105, CD90, CD29, CD73, CD71, and Stro-1 (Fig. 2A) [14,15]. Human cardiospheres also expressed both vimentin and collagen type 1 (Fig. 2B), and had a spindle shaped morphology in attached cell-culture experiments (Fig. 2C). RT-PCR showed that hCSCs expressed ATP-binding cassette transporter subfamily G member 2 (ABCG2), which was associated with Hoechst's efflux properties prerequisite for the side population cells [16]. Human cardiospheres also expressed Rex1, Nanog, and Sox2, although Oct4 was not detectable (Fig. 2D), suggesting that hCSCs express the embryonic stem cell markers and contain the mesenchymal cell-like population.

hCSCs give rise to cardiovascular lineages in vitro and in vivo

To determine the differentiation potential of hCSCs *in vitro*, hCSCs were cultured in differentiation medium. Immunostaining showed that hCSCs gave rise to smooth muscle cells, endothelial cells, and cardiomyocytes co-expressing connexin-43 (Fig. 3A). Furthermore, cardiac-specific transcriptional factors such as Nkx2.5 and GATA4, ANP, and structural genes, including α-cardiac-actin, cardiac troponin-T, MLC2a, MLC2v, α-MHC, and β-MHC, were detected in the differentiated cardiomyocytes by RT-PCR (Fig. 3B).

To investigate the regenerative potential of hCSCs *in vivo*, we performed cell transplantation into MI using NOD/*scid* mice. The injected cells formed a successful engraftment within the border and infarcted regions. The differentiation of hCSCs into the cardiovascular-lineage cells was verified by the presence of smooth muscle cells, endothelial cells, and cardiomyocytes, colocalized with human nuclei (Fig. 3C). Capillary density was also increased in the implanted hearts compared with the PBS-treated hearts (Fig. 3D).

After the transplantation of hCSCs, cardiac function was analyzed by echocardiography (Fig. 3E). In PBS-treated mice, the ejection fraction (EF) and fractional shortening (FS) were significantly decreased (EF: $81.5 \pm 2.0\%$ to $46 \pm 2.0\%$, $p < 0.01$; FS: $43.7 \pm 2.0\%$ to $20.2 \pm 1.0\%$, $p < 0.01$), and LV diastolic dimension (Dd) was expanded (35.2 ± 2.0 to 47.0 ± 3.0 mm, $p < 0.01$) at day-14 after MI compared with baseline. In contrast, the implantation of hCSCs effectively ameliorated the cardiac dysfunction (EF: $46 \pm 2.0\%$ vs $58 \pm 2.0\%$, $p < 0.01$; FS: $20.2 \pm 1.0\%$ vs $26.2 \pm 2.0\%$, $p < 0.01$) and reduced LV dilatation (Dd: $47.0 \pm 3.0\%$ vs $40.7 \pm 2.0\%$, $p < 0.01$) compared with PBS-injected mice. These parameters showed that the

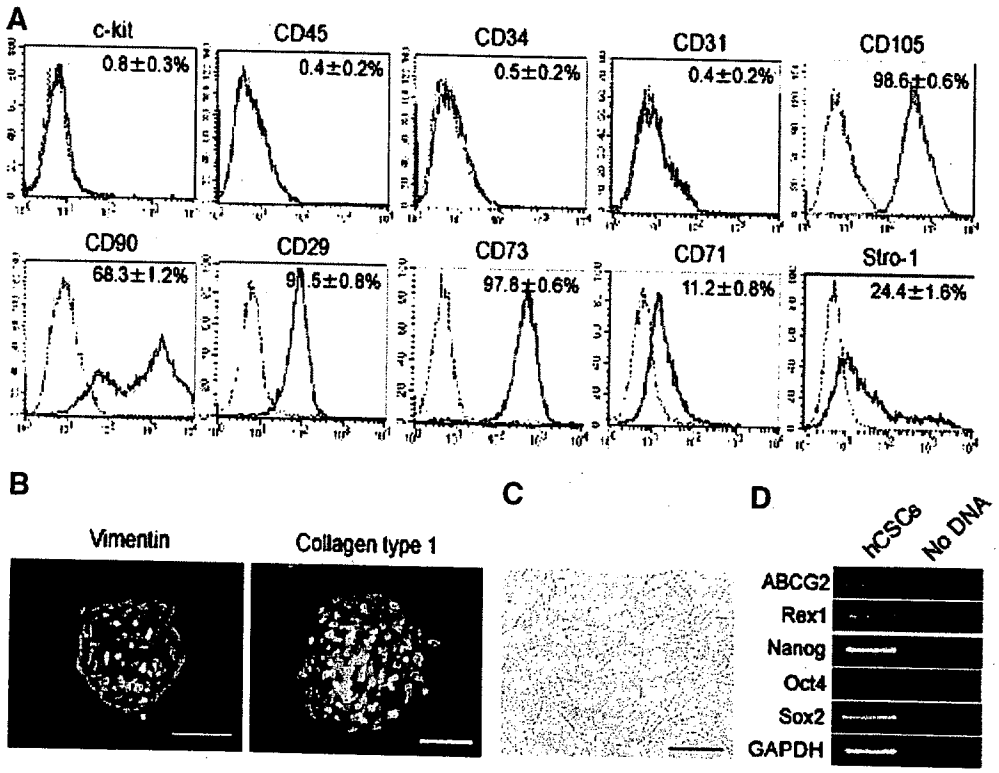

Fig. 2. Characterization of hCSCs. (A) FACS analysis of hCSCs. Black line, control IgG; red line, corresponding antibody ($n = 3$). (B) Immunostaining of human cardiospheres. Red signals show the expression of vimentin (left) and collagen typeI (right). Scale bars, 50 μm. (C) Phase contrast image of hCSCs in attached cell-culture. Scale bars, 100 μm. (D) Gene expression profile by RT-PCR examined in hCSCs. No DNA template was used as a negative control ($n = 6$).

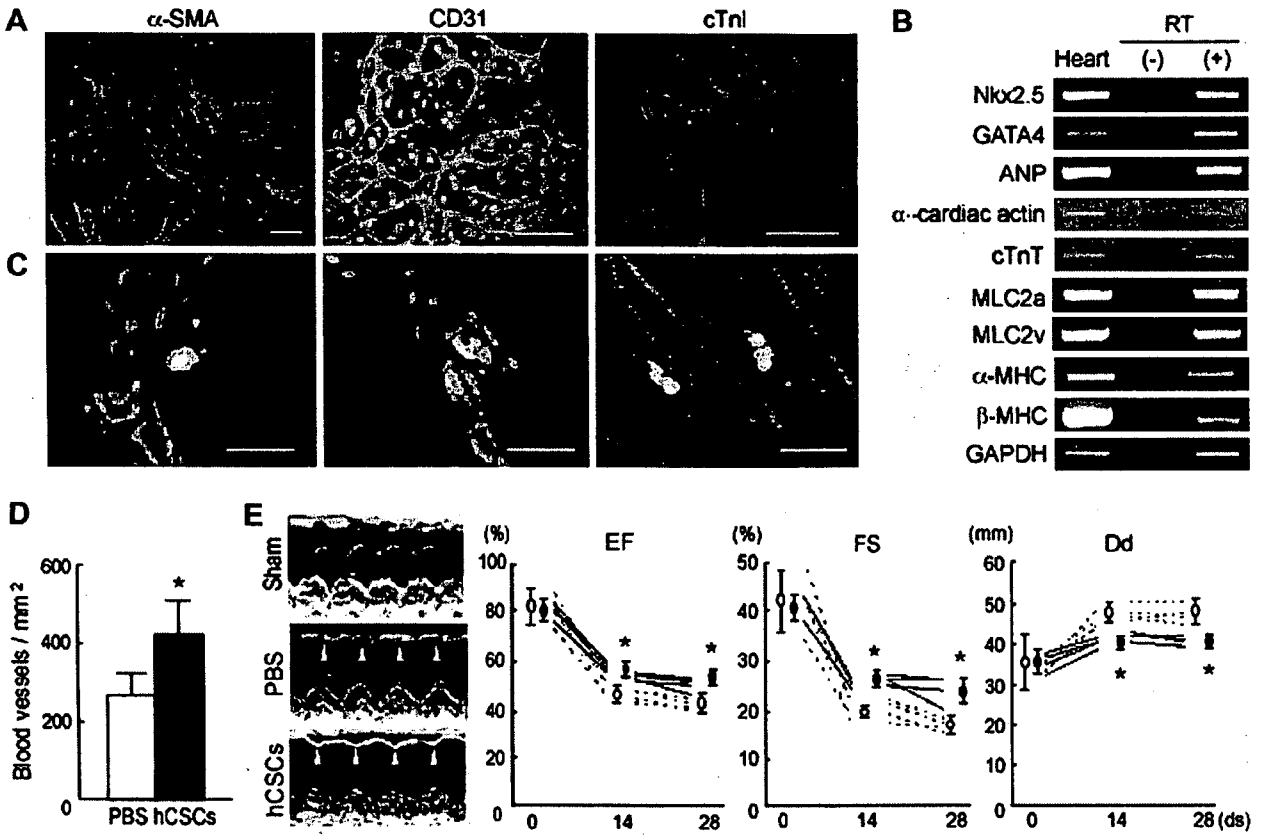

Fig. 3. Functional differentiation of hCSCs *in vitro* and *in vivo*. (A) *In vitro* differentiation of hCSCs into smooth muscle cells (left: α-SMA, red), endothelial cells (middle: CD31, green), and cardiomyocytes (right: cardiac troponin-I, red; connexin-43, yelow). DAPI, blue. (B) RT-PCR shows cardiac differentiation of hCSCs. Heart tissue was used as positive control ($n = 3$). (C) *In vivo* differentiation of hCSCs. Smooth muscle cells (left: α-SMA, red), endothelial cells (middle: CD31, red), and cardiomyocytes (right: cardiac troponin-I, red), counterstained with human nuclei (green) are shown. DAPI, blue ($n = 4$). (D) Capillary density was assessed by CD31 immunohistochemistry in the border zone. $^*p < 0.01$ versus PBS treated mice. (E) Serial assessment of cardiac function by echocardiography. Representative M-mode images of sham-operated, PBS-injected, and hCSC-transplantated hearts at 28 days after MI. Closed circles, hCSC transplanted hearts; open circles, PBS-injected hearts ($n = 8$). Arrowheads indicate significantly improved anterior wall movement on stem cell implantation. $^*p < 0.01$ versus PBS-treated mice. Scale bars, 50 μm in (A); 20 μm in (C).

significant recovery was observed 2 and 4 weeks after hCSC implantation.

The proliferation and survival of hCSCs depend on Akt/GSK-3β pathway

Akt pathway plays a crucial role to mediate the proliferation activity in mCSCs [13]. To verify whether Akt pathway was involved in hCSC proliferation, we examined the activation of Akt in hCSCs and found that EGF/bFGF treatment of hCSCs caused a rapid activation of Akt (Fig. 4A) and also augmented sustained phosphorylation of GSK-3β, which is one of the downstream targets of Akt, to inactivate GSK-3β function (Fig. 4B). The EGF/bFGF-induced activation of Akt in hCSCs was inhibited by Akt inhibitor, Akt-I, in a dose-dependent manner (Fig. 4C). In contrast, the levels of phosphorylated GSK-3β (inactive form of GSK-3β) could be enhanced by the treatment of 10 nM GSK-3-inhibitor, BIO (Fig. 4D), as previously reported in renal epithelial cells [17].

If Akt mediates hCSC proliferation through the inhibition of GSK-3β, the pharmacological inhibition of Akt/GSK-3β signaling pathways may affect the growth of hCSCs. To test this hypothesis, the diameter of cardiospheres was measured in the presence or absence of 10 μM Akt-I or 10 nM BIO, the minimal doses needed to achieve an effect shown above (Fig. 4C and D). Our results demonstrated that Akt-I significantly decreased the diameter of EGF/bFGF-expanded cardiospheres (Fig. 4E), whereas addition of BIO significantly increased their growth at the range of sphere size more than 100 μm (Fig. 4F).

We next determined the underlying mechanisms by which Akt/GSK-3β pathway modulated sphere formation and growth of hCSCs. TUNEL$^+$ cells were significantly increased in cardiospheres treated with Akt-I compared with control, whereas BIO apparently reduced the number of TUNEL$^+$ cells (Fig. 4G). In contrast, Ki67-positive cells were apparently decreased in cardiospheres treated with Akt-I compared with control, whereas a significant